uicc
global cancer control

IJC
International Journal of Cancer

Proviral loads of human T-lymphotropic virus Type 1 in asymptomatic carriers with different infection routes

Shiro Ueno[1], Kazumi Umeki[1], Ichiro Takajo[1], Yasuhiro Nagatomo[1], Norio Kusumoto[1], Kunihiko Umekita[1], Kazuhiro Morishita[2] and Akihiko Okayama[1]

[1] Department of Rheumatology, Infectious Diseases and Laboratory Medicine, Faculty of Medicine, University of Miyazaki, Miyazaki, Japan
[2] Division of Tumor and Cellular Biochemistry, Department of Medical Sciences, University of Miyazaki, Miyazaki, Japan

High human T-lymphotropic virus Type 1 (HTLV-1) proviral DNA load (PVL) has been reported to be one risk factor for the development of adult T-cell leukemia/lymphoma (ATL). ATL is also believed to develop in HTLV-1 carriers who acquire infection perinatally. ATL cells have been reported to frequently harbor defective provirus. In our study, PVLs for three different regions of HTLV-1 provirus (5′LTR-*gag*, *gag* and *pX*) were measured in 309 asymptomatic carriers with different infection routes. PVLs for the *pX* region in 21 asymptomatic carriers with maternal infection was significantly higher than in 24 carriers with spousal infection. Among 161 carriers with relatively high *pX* PVLs (equal to or greater than 1 copy per 100 peripheral blood mononuclear cells), 26 carriers (16%) had low *gag* PVL/*pX* PVL (less than 0.5) and four (2%) had low 5′LTR-*gag* PVL/*pX* PVL (less than 0.5). Low *gag* PVL/*pX* PVL ratio, which reflects deficiency and/or polymorphism of HTLV-1 proviral DNA sequences for the *gag* region, was also associated with maternal infection. These data suggest that HTLV-1 carriers with maternal infection tend to have high PVLs, which may be related to provirus with deficiency and/or the polymorphism of proviral DNA sequences. In addition, there is a possibility that this ratio may be used as a tool to differentiate the infection routes of asymptomatic HTLV-1 carriers, which supports the need for a large scale study.

Human T-lymphotropic virus Type 1 (HTLV-1) is the causative agent of adult T-cell leukemia/lymphoma (ATL) and a progressive neurological disease known as HTLV-1-associated myelopathy/tropical spastic paraparesis (HAM/TSP).[1–4] Major routes of HTLV-1 infection have been reported as mother to child infection at infancy, sexual contact between spouses and blood transfusion.[5–7] The majority of HTLV-1 carriers are asymptomatic, and only a fraction of carriers develop ATL after a long latent period.[8,9] It has been reported that approximately 4% of HTLV-1 carriers develop ATL eventually.[10] Studies of the mothers of patients with ATL have reported most of them to be HTLV-1 carriers.[11,12] Therefore, ATL is believed to develop in HTLV-1 carriers who acquire infection perinatally. However, there has been no method of identifying the infection route of HTLV-1 positive individuals without information on family HTLV-1 status.

When an individual is infected by HTLV-1, the virus randomly integrates into the genome of affected T-cells in the form of provirus.[13] HTLV-1 infection drives the proliferation of T-cells, leading to the clonal expansion of HTLV-1 infected cells.[14–16] Recently, it was reported that HTLV-1 clonal expansion *in vivo* is favored by orientation of the provirus in the same sense as the nearest host gene.[17] We have reported that the clonality of HTLV-1 infected cells in adult seroconverters who were newly infected from HTLV-1 carrier spouses is more heterogeneous and less stable than that of long-term carriers who acquired infection from their mothers at infancy.[18] The selective maintenance of certain clones is supposed in the latter. Recently, we reported that clonal expansion of HTLV-1 infected cells was found in a certain population of asymptomatic carriers and that these carriers had high proviral DNA loads (PVLs).[19] High PVLs have been reported to be a risk factor for developing ATL.[20,21] In another study, we analyzed the PVLs of 13 pairs of HTLV-1 seroconverters and their spouses.[22] Although seroconverters and their spouses shared the same HTLV-1, PVLs in both individuals in a couple were not always equivalent. These findings suggested that host-related factors play an important role to determining the PVL in each carrier. However, it was

Key words: HTLV-1, defective virus, infection route, proviral DNA loads

Abbreviations: ATL: adult T-cell leukemia/lymphoma; HTLV-1: human T-lymphotropic virus type 1, LTR: long-terminal repeat, PBMCs: peripheral blood mononuclear cells, PCR: polymerase chain reaction; PVLs: proviral DNA loads

Grant sponsors: Ministry of Education, Science, Sports and Culture, Japan, Miyazaki Prefecture Collaboration of Regional Entities for the Advancement of Technological Excellence, JST
DOI: 10.1002/ijc.26289
History: Received 22 Feb 2011; Accepted 16 Jun 2011; Online 21 Jul 2011

Correspondence to: Akihiko Okayama, Department of Rheumatology, Infectious Diseases and Laboratory Medicine, Faculty of Medicine, University of Miyazaki, 5200 Kihara, Kiyotake, Miyazaki 889-1692, Japan, Tel.: 81-985-85-7284
Fax: 81-985-85-4709, E-mail: okayama@med.miyazaki-u.ac.jp

not clear in that study whether HTLV-1 carriers who acquired infection from their mothers at infancy have more PVLs than the carriers who acquired infection from their spouses in adulthood.

Defective provirus has frequently been detectable in patients with ATL.[23–27] The complete HTLV-1 provirus is approximately 9 kb and contains the coding regions for core protein (*gag*), protease (*pro*), polymerase (*pol*), envelope protein (*env*), regulatory proteins, such as Tax and Rex, and some accessory molecules between 5′ and 3′ long-terminal repeats (LTRs).[8,28] Tamiya *et al.*[23] reported two types of genome deletion in defective provirus. One form retains both LTRs and lacks internal sequences, such as the *gag* and *pol* regions. The other form has the 3′ LTR, and the 5′ LTR and its flanking internal sequences are preferentially deleted. HTLV-1 infected cells harboring the latter defective virus were frequently found in patients with ATL.[26] Both types of defective provirus were suspected of being harbored by the clonally expanded HTLV-1 infected cells in asymptomatic carriers.[19] The polymorphism of the proviral genome was also found in asymptomatic carriers in that study; however, we could not show how commonly the deficiency or polymorphism of the proviral genome was detectable.

These questions prompted us to investigate HTLV-1 PVLs in asymptomatic carriers with different infection routes. In addition, to clarify whether the defective provirus and/or polymorphism of the proviral genome affected PVLs, we tested PVLs for three different regions (5′LTR-*gag*, *gag* and *pX*) of provirus in each individual and compared them among the carriers with different infection routes in our study.

Material and Methods

Samples

Samples of peripheral blood mononuclear cells (PBMCs) were obtained from 309 HTLV-1 carriers (103 men and 206 women, median age: 67 years), who had no symptoms or laboratory data suggesting HTLV-1 related disease, in the Miyazaki Cohort Study.[29] Infection routes were investigated by family HTLV-1 status and history of HTLV-1 seroconversion.[18,22] An HTLV-1 carrier with HTLV-1 positive mother/HTLV-1 negative spouse or with HTLV-1 positive siblings/HTLV-1 negative spouse or with HTLV-1 seroconverter was defined as infected by his/her mother. An HTLV-1 carrier who was a HTLV-1 seroconverter with HTLV-1 positive spouse or with HTLV-1 negative mother/HTLV-1 positive spouse was defined as infected by his/her spouse. Carriers with history of blood transfusion were excluded from the analysis of family status. As a result, 21 and 24 carriers were defined as infected by their mothers and by their spouses, respectively. Infection routes could not be determined in 264 carriers. Informed consent was obtained from the study participants and the study protocol was approved by the institutional review board at University of Miyazaki.

Real-time polymerase chain reaction

PVLs for three different proviral regions (5′LTR-*gag*, *gag* and *pX*) were determined by real-time polymerase chain reaction (PCR) using Light Cycler 2.0 (Roche Diagnostics, Mannheim, Germany). Genomic DNA was isolated from PBMCs of asymptomatic HTLV-1 carriers by sodium dodecyl sulfate-proteinase K digestion, followed by phenol-chloroform extraction and ethanol precipitation. Approximately 100 ng genomic DNA was used as the template. The nucleotide position number of HTLV-1 provirus was according to Seiki *et al.*[30] (accession no. J02029). The primers and probes for real-time PCR were designed to minimize the differences of the melting points 5′LTR-*gag*, *gag* and *pX* and were as follows: 5′LTR-*gag*: the forward primer (5′LTR-SDS-F 5′-AAGTACCGGCGACTCCGTTG-3′: positions 700–719), the reverse primer (HTLV-gag-LTR-R2 5′-GGCTAGCGCTACGGGAAAAG-3′: positions 854–835) and the FAM-labeled probe (5′-FAM-CGTCCGGGATACGAGCGCCCCTT-TAMRA-3′: positions 788–810); *gag*: the forward primer (HTLV-gag-F5 5′-ACCCTTCCTGGGCCTCTATC-3′: positions 1,602–1,621), the reverse primer (HTLV-gag-R5 5′-TCTGGCAGCCCATTGTCAAG-3′: positions 1,695–1,676) and the FAM-labeled probe (HTLV-gag-P5 5′-FAM-ACCACGCCTTCGTAGAACGCCTCAAC-TAMRA-3′: positions 1,644–1,669); *pX*: the forward primer (HTLV-pX2-S 5′-CGGATACCCAGTCTACGTGTT-3′: positions 7,359–7,379), the reverse primer (HTLV-pX2-AS 5′-CAGTAGGGCGTGACGATGTA-3′: positions 7,458–7,439) and the FAM-labeled probe (HTLV-pX2-Probe 5′-FAM-CTGTGTACAAGGCGACTGGTGCC-TAMRA-3′: positions 7,386–7,408).[18,26] A coding region for albumin (*Alb*) was used to measure the copy number of human genome. The primers and the probe for the *Alb* were as follows: The forward primer (Alb-S2 5′-TGTCATCTCTTGTGGGCTGT-3′), the reverse primer (Alb-AS2 5′-GGTTCTCTTTCACTGACATCTGC-3′) and the FAM-labeled probe (Alb-probe 5′-FAM-CCTGTCATGCCCACACAAATCTCTCC-TAMRA-3′). A plasmid containing PCR products for HTLV-1 5′LTR-*gag*, *gag*, *pX* regions and *Alb* was constructed using pGEM T-Easy Vector (Promega Corporation, Madison, WI) and was used as a control template for real-time PCR. PVLs of each region of HTLV-1 provirus were measured in a duplicate manner and were shown as copies per 100 PBMCs.

Detection of provirus with deletion of HTLV-1 internal sequence by long PCR

To detect the provirus with large deletion of HTLV-1 internal sequence, long PCR, which amplifies provirus maintaining both 5′ and 3′ LTR, was performed as described previously.[19] The primers were as follows: 5′LTR (HTLV-0647F 5′-GTTCCACCCCTTTCCCTTTCATTCACGACTGACTGC-3′: positions 647–682) and 3′LTR (HTLV-8345R 5′-GGCTCT AAGCCCCCGGGGGATATTTGGGGCTCATGG-3′: positions

8,345–8,310).[26] Long PCR was performed using LA Taq Hot start version (Takara Bio, Shiga, Japan). Genomic DNA containing 200 copies of HTLV-1 provirus for the *pX* region was used for this assay. To ensure that the same amount of provirus was used in each reaction, PCR for the *pX* region was performed as an internal control. Primers for this PCR were as follows: the forward primer (HTLV-7396F 5′-GGCGACTGGTGCCCCATCTCTGGGGGACTATGTTCG-3′: positions 7,396–7,431) and the reverse primer described above (HTLV-8345R). The PCR products were electrophoresed on 0.8% agarose gel and visualized by ethidium bromide staining.

Detection of provirus with deletion of 5′LTR and its flanking internal sequence by inverse long PCR

As described in results, both *gag* PVL/*pX* PVL ratio and 5′LTR-*gag* PVL/*pX* PVL ratio were low at less than 0.5 in two carriers (C20 and 21) and they were suspected of having provirus with deletion of 5′LTR and its flanking internal sequence. Inverse long PCR (IL-PCR) was used to amplify the genomic DNA adjacent to the 3′LTR of HTLV-1 provirus according to the method described previously with slight modifications.[15] In brief, the genomic DNA was digested with *Kpn* I, *Hind* III, *Sal* I or *Spe* I, and then self-ligated by T4 ligase following digestion with *Mlu* I. Amplification of the resultant DNA was performed using the LA Taq Hot start version. The primers used in this analysis were as follows; a forward primer in the U5 region of the LTR (5′-TGCCTGACCCTGCTTGCTCAACTCTACGTCTTTG-3′: positions 8,856–8,889) and a reverse primer, HTLV-7002R (5′-AGTATTTGAAAAGGAAGGAAGAGGAGAAGGCA-3′: positions 7,002–6,971). Subcloning of the amplified fragments of IL-PCR were subjected to sequencing assay according to the protocol of the Big Dye Terminator v1.1 Cycle Sequencing Kit (Applied Biosystems, Foster City, CA) using ABI Prism 310 DNA Sequencer (Applied Biosystems) and the human genomic sequence downstream of the HTLV-1 provirus was obtained. The human genomic sequence upstream of the provirus was assumed based on this information by BLAT search (http://genome.ucsc.edu/cgi-bin/hgBlat).[31] The primers for human genomic sequence upstream of the provirus were designed and long PCR was performed using a forward primer (5′-GTGATCCATGGTGTTTGTCCACCTGAAAGC-3′) and a reverse primer HTLV-7002R in C20, and a forward primer (5′-TCCAAGTGGGATGTCACGGCCACTTCTC-3′) and a reverse primer HTLV-7002R in C21. To determine the upstream junction sequence between host genome and provirus, the PCR products were subjected to direct sequencing using the Big Dye Terminator v1.1 Cycle Sequencing Kit.

Statistical Analysis

Mann-Whitney's U test was used to compare *pX* PVLs, *gag* PVL/*pX* PVL or 5′LTR-*gag*/*pX* PVL ratios among the groups of asymptomatic HTLV-1 carriers with different infection routes. Spearman's correlation coefficient by rank was used to determine the relationship between *pX* PVL and *gag* PVL/*pX* PVL or 5′LTR-*gag* PVL/*pX* PVL ratio.

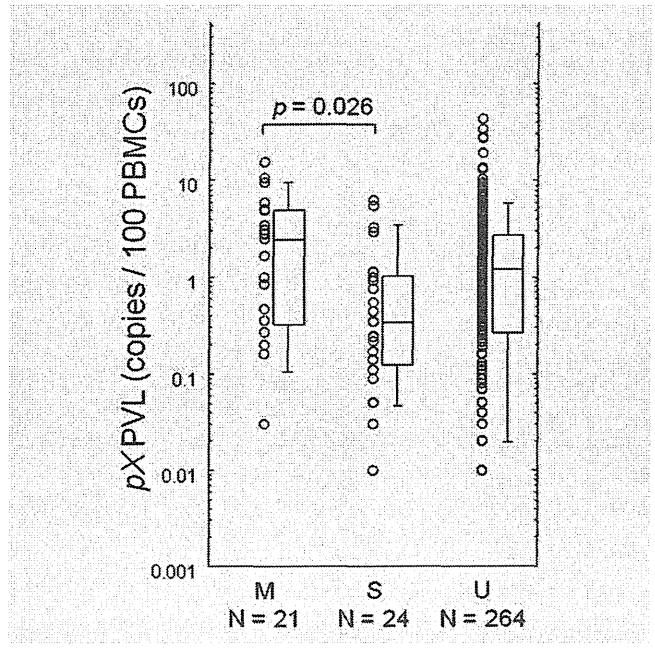

Figure 1. *PX* PVLs in HTLV-1 carriers with different infection routes M: Carriers with infection from mothers; S: Carriers with infection from spouses; U: Carriers with undetermined infection routes.

Results

pX PVLs in HTLV-1 carriers with different infectious routes

PVLs for the 5′LTR-*gag*, *gag* and *pX* regions in each individual were measured in 309 asymptomatic HTLV-1 carriers. Because the *pX* region has been reported to be conserved in the HTLV-1 provirus, *pX* PVL was considered to represent total PVLs.[23,25] As shown in Figure 1, median *pX* PVL (2.49 copies/100 PBMCs) in 21 asymptomatic carriers, who were infected by their mothers, was significantly higher than that (0.34 copies/100 PBMCs) in 24 carriers who were infected by their spouses ($p = 0.026$). Median *pX* PVL in 264 asymptomatic carriers, whose infection routes were undetermined, was between these values (1.24 copies/100 PBMCs).

PVLs for 3 different proviral regions (5′LTR-gag, gag and pX) of HTLV-1

To determine whether PVLs for three different proviral regions (5′LTR-*gag*, *gag* and *pX*) of HTLV-1 were equal in asymptomatic carriers, PVLs for the 5′LTR-*gag* and *gag* regions were measured and compared to PVLs for the *pX* region. Because 100 ng of genomic DNA, which is derived approximately 15,000 PBMCs, was used for the template for real time-PCR, 148 carriers with *pX* PVL, which was less than 1 copy/100 PBMCs, were not provided for further analysis to avoid unstable result due to the small number of proviral copies in each reaction. The results of our study were

shown as the ratio of PVLs for the 5′LTR-*gag* or *gag* regions to PVL for the *pX* region in each individual (Fig. 2). The median 5′LTR-*gag* PVL/*pX* PVL ratio of 161 HTLV-1 carriers tested was 0.97. Therefore, HTLV-1 proviral sequence for 5′LTR-*gag* PVL was considered to be conserved in the majority of asymptomatic carriers. The median *gag* PVL/*pX* PVL ratio, however, was 0.61.

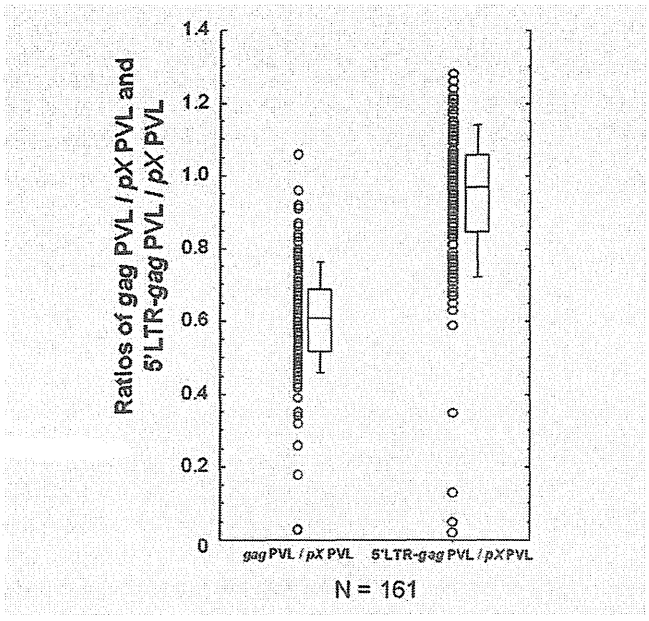

Figure 2. The ratios of PVLs for the 5′LTR-*gag* or *gag* regions to PVL for the *pX* region in 161 asymptomatic HTLV-1 carriers, whose *pX* PVLs were equal to or greater than 1 copy/100 PBMCs.

Detection of provirus with deletion of HTLV-1 internal sequence by long PCR

To determine whether the provirus with deletion of HTLV-1 internal sequence accounted for low *gag* PVL/*pX* PVL ratio, long PCR was performed. For this analysis, we chose 26 carriers with low *gag* PVL/*pX* PVL ratios of less than 0.5; however, adequate DNA sample for long PCR was available in only 17 of the 26 subjects. All subjects except C1 showed a band of 7.7 kb, which was considered to be derived from complete provirus, and some additional smaller bands suggesting defective provirus (Fig. 3*a*). C1 showed only a dense band of 4.5 kb. C1 was analyzed in our previous study and a large deficiency (3.2 kb, positions 1,203–4,368) of internal sequence was shown.[19] Additional four carriers (C3, 4, 11 and 13) showed dense bands equal to or stronger than the band for complete provirus (arrows in Fig. 3*a*). Cloning and DNA sequencing of these dense bands showed large deficiencies of internal sequences (4.9 kb, positions 1,368–6,286 in C3; 0.9 kb, positions 1,413–2,284 in C4; 4.8 kb, positions 1,009–5,763 in C11 and 4.8 kb, positions 1,133–5,974 in C13).

Four carriers (C18–21) had low 5′LTR-*gag* PVL/*pX* PVL ratios of less than 0.5. Long PCR of C18 and 19 showed dense bands of 7.7 kb, which were considered to be derived from complete provirus, and some additional smaller bands (Fig. 3*b*). Polymorphism of proviral DNA sequence of the sites for primers and/or probe for 5′LTR-*gag* PVL was suspected in these two cases, and cloning and DNA sequencing of the PCR products were performed. The polymorphisms of DNA sequence for the annealing site of the forward primer (708 G > A and 709 C > G in C18; 712 C > T in C19) were consistently found, and these polymorphisms were

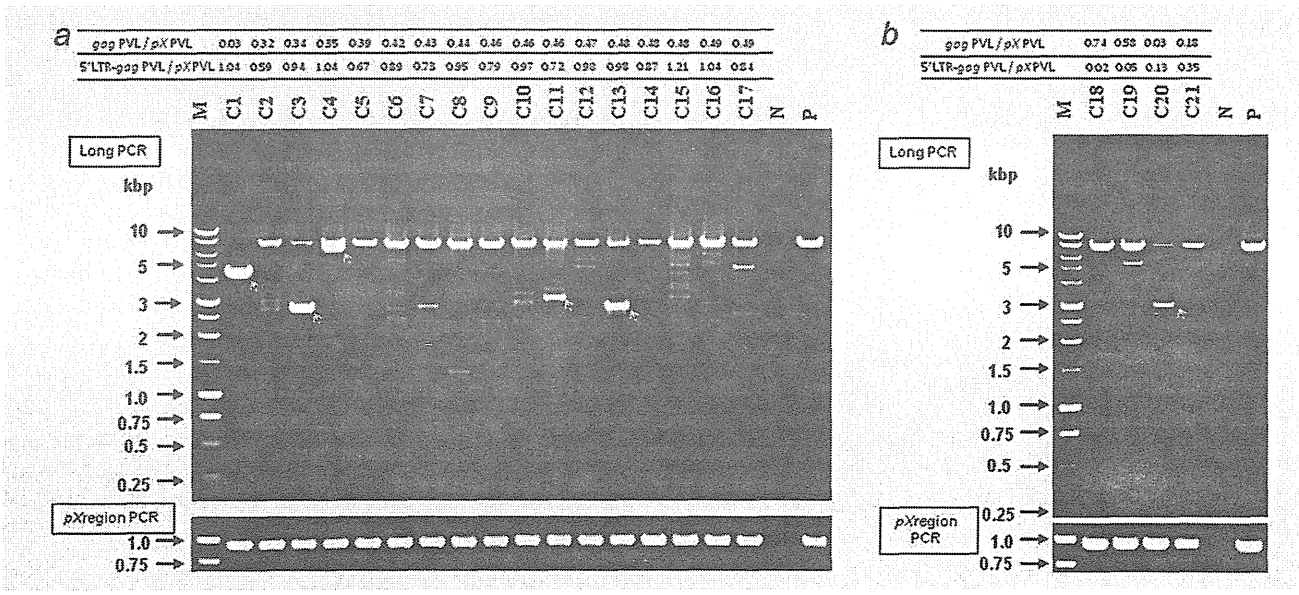

Figure 3. Detection of defective provirus by long PCR. (*a*) Asymptomatic HTLV-1 carriers with low *gag* PVL/*pX* PVL ratios less than 0.5. (*b*) Asymptomatic HTLV-1 carriers with low 5′LTR-*gag* PVL/*pX* PVL ratios less than 0.5. Arrows indicate PCR products for HTLV-1 provirus lacking large internal sequence. M: Molecular weight marker; N: HTLV-1-negative subject; P: HTLV-1-positive cell line, ED-40515(-).

considered to account for the decreased efficacy of real time-PCR for 5′LTR-*gag* PVL.

Detection of provirus with deletion of 5′LTR and its flanking internal sequence by IL-PCR

Both *gag* PVL/*pX* PVL ratio and 5′LTR-*gag* PVL/*pX* PVL ratio were low at less than 0.5 in the additional two carriers (C20 and 21). Long PCR showed a weak band of 7.7 kb for complete provirus and a stronger band of 2.9 kb in C20 (Fig. 3*b*). In the case of C21, only a weak band for complete band was observed (Fig 3*b*). These data suggested defective provirus, which had not been detected by long PCR, existed in C20 and C21. Because these proviruses were suspected of lacking 5′LTR and its flanking internal sequence, we attempted to identify them by IL-PCR. First, the genomic DNA of C20 and C21 were digested with *Kpn* I, *Hind* III, *Sal* I or *Spe* I, and resultant DNA was provided for IL-PCR as a template. In C20, approximately 1.1 kb of PCR product was obtained in digestion with *Kpn* I alone (Fig. 4*a-1*). No IL-PCR product was obtained using other restriction enzymes (data not shown). When this PCR product was digested with *Kpn* I, two major bands appeared, as expected (Fig. 4*a-1*). Cloning and sequencing revealed that this product consisted of HTLV-1 provirus (*Kpn* I site at position: 6,141 to the end of 3′LTR) and its flanking genomic DNA of human chromosome 2 (2q13). Based on the information obtained, a forward primer to anneal the upstream human genome adjuncted to the provirus was prepared and clone-specific PCR was performed. Cloning and sequencing of this clone-specific PCR product revealed that it lacked 5′LTR and its internal flanking sequence (until position 5,999; Fig. 4*a-2*). In the case of C21, IL-PCR product was obtained in digestion with *Hind* III alone. Following the same procedure as in C20, it was revealed that a provirus integrated in human chromosome 18 (18p11.32), and that it lacked 5′LTR and its internal flanking sequence (until position 4,976) (Figs. 4*b-1* and 4*b-2*).

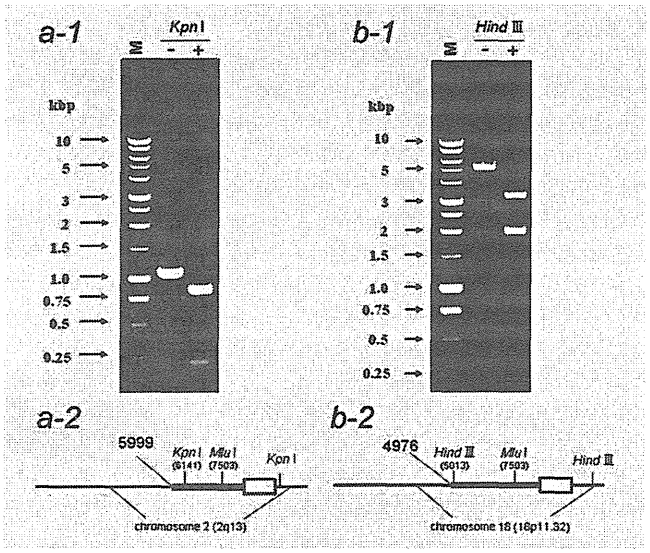

Figure 4. Detection of provirus with deletion of 5′LTR and its internal flanking sequence by IL-PCR. (*a-1*) Long PCR products from an asymptomatic HTLV-1 carrier, C20, with or without *Kpn* I digestion. (*a-2*) Scheme of the structure of defective provirus in C20. (*b-1*) Long PCR products from an asymptomatic HTLV-1 carrier, C21, with or without Hind III digestion. (*b-2*) Scheme of the structure of defective provirus in C21.

Relationship between pX PVL and gag PVL/pX PVL or 5′LTR-gag/pX PVL ratios

To determine whether the HTLV-1 PVLs correlated with the number of provirus with deficiency and/or polymorphism of the *gag* or 5′LTR-*gag* regions, the relationship between *pX* PVL and *gag* PVL/*pX* PVL or 5′LTR-*gag*/*pX* PVL ratios was analyzed. As shown in Figure 5*a*, there was a negative

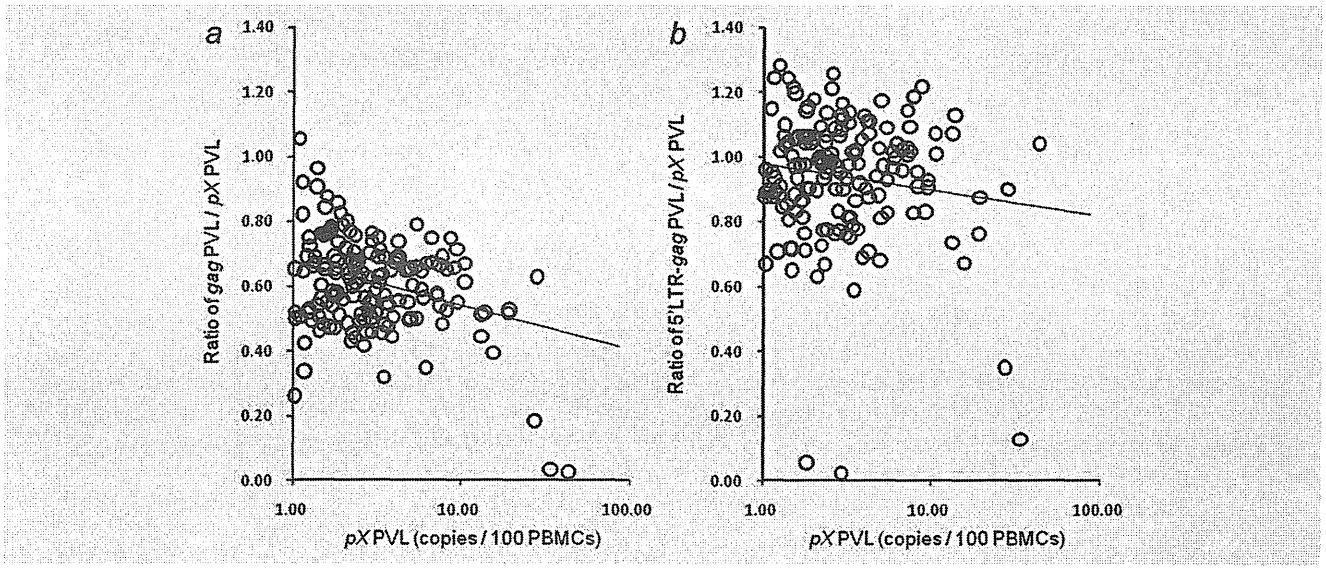

Figure 5. Relations of *pX* PVL and *gag* PVL/*pX* PVL or 5′LTR-*gag* PVL/*pX* PVL ratios in 161 asymptomatic carriers. (*a*) Relation of *pX* PVL and *gag* PVL/*pX* PVL. (*b*) Relation of *pX* PVL and 5′LTR-*gag* PVL/*pX* PVL.

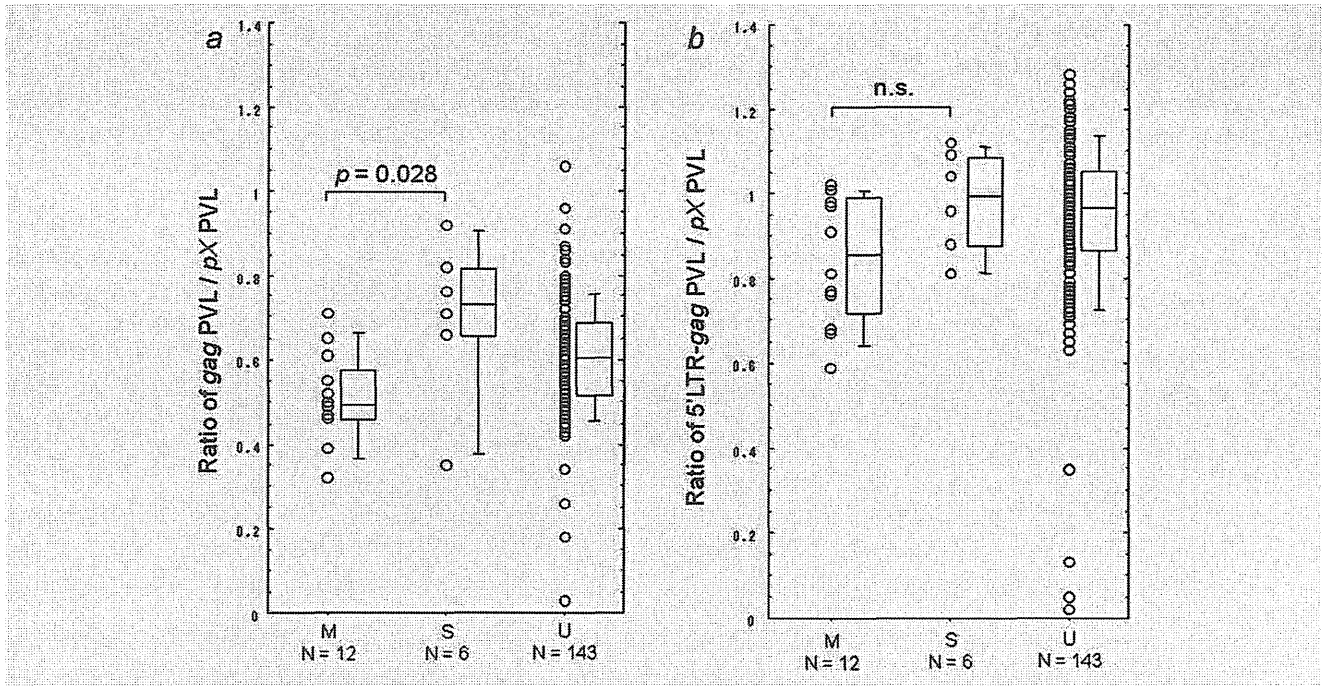

Figure 6. The ratios of *gag* PVL/*pX* PVL or 5′LTR-*gag* PVL/*pX* PVL in HTLV-1 carriers with different infection routes in 161 asymptomatic carriers. (*a*) The ratio of *gag* PVL/*pX* PVL. (*b*) The ratio of 5′LTR-*gag* PVL/*pX* PVL. M: Carriers with infection from mothers; S: Carriers with infection from spouses; U: Carriers with undetermined infection routes.

correlation between *pX* PVL and the *gag* PVL/*pX* PVL ratio ($r = -0.46$, $p = 0.02$). Therefore, HTLV-1 infected cells harboring provirus with deficiency and/or polymorphism of the *gag* region were considered to be more prevalent in asymptomatic carriers with high PVL. In the case of 5′LTR-*gag*/*pX* PVL ratio, the trend was not obvious (Fig. 5*b*) ($r = -0.20$, $p = 0.94$). However, variability of the 5′LTR-*gag*/*pX* PVL ratio was greater than that of *gag* PVL/*pX* PVL ratio. This may have been the result of technical inadequacies in the measurement of 5′LTR-*gag* PVL.

The ratios of gag PVL/pX PVL and 5′LTR-gag PVL/pX PVL in HTLV-1 carriers with different infection routes

Next, the relationships between infection routes and the *gag* PVL/*pX* PVL or 5′LTR-*gag*/*pX* PVL ratios were analyzed. The median ratio of *gag* PVL/*pX* PVL in 12 HTLV-1 carriers with maternal infection (0.50) was significantly lower than that in six carriers with spousal infection (0.74) ($p = 0.028$) (Fig. 6*a*). The median *gag* PVL/*pX* PVL ratio of 143 carriers with undetermined infection route (0.62) was between these. The 5′LTR-*gag* PVL/*pX* PVL ratio did not reveal a significant difference between the carriers with maternal infection and spousal infection (Fig. 6*b*). Therefore, the carriers with maternal infection were considered to have a greater number of HTLV-1 infected cells harboring provirus with deficiency and/or polymorphism of the *gag* region. In addition, when a *gag* PVL/*pX* PVL ratio of 0.65 was used as cut-off value, 11 of 12 (92%) carriers with maternal infection, against only one of six (17%) carriers with spousal infection, showed lower values.

Discussion

First, HTLV-1 PVLs in asymptomatic carriers with different infection routes were analyzed. *PX* PVL in 21 asymptomatic carriers with maternal infection was significantly higher than that in 24 carriers with spousal infection. These results agreed with data reported by Roucoux *et al.*[32] showing that PVLs in index HTLV-1 positive carriers were higher than those of their newly infected partners. Asymptomatic carriers whose infection routes were undetermined showed values between these. Previously, we analyzed the PVLs of HTLV-1 seroconverters and their spouses and showed that PVLs were not equivalent between them.[22] Because HTLV-1 in a seroconverter and in his/her spouse is identical, the host factor was considered important in the determination of HTLV-1 PVL. The results of our study suggest that infection route and/or time of infection are factors in the determination of PVL in HTLV-1 carriers. We also reported that HTLV-1 carriers who developed ATL had high PVLs even before they developed the disease.[20] Recently, Iwanaga *et al.*[21] also tested the PVLs of 1,218 HTLV-1 carriers and found that HTLV-1 carriers that developed ATL had high PVLs. These data suggest that high HTLV-1 PVL is a risk factor for developing ATL. In our study, HTLV-1 carriers with maternal infection tended to have high PVLs. This may account for why perinatal infection is a risk factor of ATL at least in part.

Because the frequent detection of defective provirus in patients with ATL has been reported, we examined provirus with deficiencies and/or polymorphism of proviral sequence in asymptomatic HTLV-1 carriers. The *pX* region has been

reported to be conserved in HTLV-1 provirus, and PCR for this region was used to measure total PVL.[23,25] Ohshima *et al.*[25] reported that variation of DNA sequence is frequently detected in the *gag* region of HTLV-1 provirus in patients with ATL. Kamihira *et al.*[24] also reported that most of deficient provirus in patients with ATL lacked part of the *gag* region in the proviral regions of HTLV-1 tested. HTLV-1 provirus with deletion of the 5′LTR, and its flanking internal sequences was also found in patients with ATL.[26] In our study, therefore, we tried to find provirus with deficiencies and/or polymorphism of DNA sequence in the asymptomatic carriers by measuring PVLs for the *gag* and 5′LTR-*gag* regions as ratios to *pX* region PVLs. As a result, median 5′LTR-*gag* PVL/*pX* PVL and *gag* PVL/*pX* PVL ratios of 161 HTLV-1 carriers with relatively high *pX* PVL (equal to or greater than one copy per 100 PBMCs) were 0.97 and 0.61, respectively. Our interpretation of this result was that many HTLV-1 infected cells in asymptomatic carriers harbor provirus with deficiency and/or polymorphism of DNA sequences for the sites of primers and/or probe for *gag* real time-PCR.

Long PCR analysis was performed on 17 carriers with low *gag* PVL/*pX* PVL ratios. Five of 17 carriers (29%) were shown to have the provirus with large deletions of internal DNA sequence including the *gag* region. The clonal expansion of HTLV-1 infected cells harboring defective provirus in these five carriers was most likely. In fact, clonal expansion of HTLV-1 infected cells in C1 was already shown in our previous study.[19] The reason for the low *gag* PVL/*pX* PVL ratios in the other 12 carriers was not clear. Contribution of the sum total of HTLV-1 infected cells with defective provirus, which did not reveal dense bands, was possible. Alternatively, polymorphism of the proviral DNA sequence for the *gag* region may have decreased the efficiency of real time-PCR for *gag* PVL. However, cloning and DNA sequencing of the sites for primers and probes for real time-PCR for *gag* PVL in these carriers did not show consistent polymorphism of the proviral DNA (data not shown). This may be because there is high diversity of proviral DNA sequence in the *gag* region of HTLV-1 and it was not possible to prepare cloning primers to work for all of them.

The other two (C20 and 21) showed low ratios not only of 5′LTR-*gag* PVL/*pX* PVL but also of *gag* PVL/*pX* PVL. Our previous study showed that they had high PVLs and clonal expansion of HTLV-1 infected cells with defective provirus.[19] We could not identify the type of defective provirus in the previous study. In our study, however, we found provirus lacking 5′LTR and its internal flanking region existed in these carriers.

In our study, the provirus with deficiency and/or polymorphism of the *gag* region was commonly found in asymptomatic HTLV-1 carriers. Few carriers had provirus lacking 5′LTR and its flanking sequence. Carriers with provirus with deficiency and/or polymorphism of the *gag* region were found frequently among asymptomatic carriers with high PVLs. These infected cells may not express certain HTLV-1 proteins. This change may make it possible for the HTLV-1 infected cells to avoid attack by cytotoxic T-lymphocytes.[33] Therefore, there is a possibility that provirus with deficiency and/or polymorphism of HTLV-1 provirus contributes to the survival of HTLV-1 infected cells. Indeed, our previous study showed that C1, 20 and 21 had clonal expansion of HTLV-1 infected cells.[19]

Low *gag* PVL/*pX* PVL ratio was found to be associated with maternal infection. The reason carriers with maternal infection have a greater number of HTLV-1 infected cells harboring provirus with deficiency and/or polymorphism of the *gag* region was not clear in our study. The replication of HTLV-1 infected cells in long-term infected carriers may account for this. Alternatively, a low level of new cell to cell infection *in vivo* can contribute to the creation of deficiency and/or polymorphism in proviral genome.

Maternal infection has been considered to be a risk factor for the development of ATL in asymptomatic carriers. However, there has been no method to identify infection route in the absence of information on family HTLV-1 status. The results of our study suggest the possibility that *gag* PVL/*pX* PVL ratio can be used as a tool to differentiate the infection routes of asymptomatic HTLV-1 carriers. Due to the fact that only a small number of HTLV-1 carriers with known infectious routes were analyzed in our study, further study with a larger number of subjects is necessary.

A major limitation of our study is that the subjects were elderly individuals, whose median age was 67 years old. The average age at onset of ATL was reported as 60 years.[34] Therefore, it is not clear whether the same result would be obtained from an analysis of younger HTLV-1 asymptomatic carriers. In addition, carriers with low *pX* PVL (less than 1 copy/100 PBMCs) were not provided for the analysis of deficiency and/or polymorphism of HTLV-1 proviral sequence because of technical limitations. Further analysis of carriers with low PVLs using improved methodology is necessary.

In conclusion, our study showed that *pX* PVL in carriers with maternal infection was significantly higher than that in carriers with spousal infection. Low *gag* PVL/*pX* PVL ratio reflecting deficiency and/or polymorphism in proviral genome was associated with high PVLs and maternal infection. These data suggest that development of ATL in carriers with maternal infection may be due in part to high PVL, which can be related to provirus with deficiency and/or polymorphism in proviral genome. In addition, *gag* PVL/*pX* PVL ratio has potential for use as a tool to differentiate infection routes of asymptomatic HTLV-1 carriers. Further study is necessary to clarify the mechanism of deficiency and/or polymorphism in HTLV-1 proviral genome and its implications in ATL development.

Acknowledgements

The authors thank Ms. Y. Kaseda and Ms. N. Kanemaru (Miyazaki University) for their technical assistance and Dr. M. Maeda (Kyoto University) for the gift of the HTLV-1 infected cell line, ED-40515(-).

References

1. Uchiyama T, Yodoi J, Sagawa K, Takatsuki K, Uchino H. Adult T-cell leukemia: clinical and hematologic features of 16 cases. *Blood* 1977;50:481–92.
2. Yoshida M, Miyoshi I, Hinuma Y. Isolation and characterization of retrovirus from cell lines of human adult T-cell leukemia and its implication in the disease. *Proc Natl Acad Sci USA* 1982;79: 2031–5.
3. Osame M, Usuku K, Izumo S, Ijichi N, Amitani H, Igata A, Matsumoto M, Tara M. HTLV-I associated myelopathy, a new clinical entity. *Lancet* 1986;1: 1031–2.
4. Gessain A, Barin F, Vernant JC, Gout O, Maurs L, Calender A, de The G. Antibodies to human T-lymphotropic virus type-I in patients with tropical spastic paraparesis. *Lancet* 1985;2: 407–10.
5. Hino S, Yamaguchi K, Katamine S, Sugiyama H, Amagasaki T, Kinoshita K, Yoshida Y, Doi H, Tsuji Y, Miyamoto T. Mother-to-child transmission of human T-cell leukemia virus type 1. *Jpn J Cancer Res (Gann)* 1985;76:474–80.
6. Kajiyama W, Kashiwagi S, Ikematsu H, Hayashi J, Nomura H, Okochi K. Intrafamilial transmission of adult T cell leukemia virus. *J Infect Dis* 1986;154: 851–7.
7. Okochi K, Sato H, Hinuma Y. A retrospective study on transmission of adult T cell leukemia virus by blood transfusion: seroconversion in recipients. *Vox Sang* 1984;46:245–53.
8. Arisawa K, Soda M, Endo S, Kurokawa K, Katamine S, Shimokawa I, Koba T, Takahashi T, Saito H, Doi H, Shirahama S. Evaluation of adult T-cell leukemia/ lymphoma incidence and its impact on non-Hodgkin lymphoma incidence in southwestern Japan. *Int J Cancer* 2000;85: 319–24.
9. Yamaguchi K, Watanabe T. Human T lymphotropic virus type-I and adult T-cell leukemia in Japan. *Int J Hematol* 2002; 76(Suppl 2):240–5.
10. Murphy EL, Hanchard B, Figueroa JP, Gibbs WN, Lofters WS, Campbell M, Goedert JJ, Blattner WA. Modelling the risk of adult T-cell leukemia/lymphoma in persons infected with human T-lymphotropic virus type I. *Int J Cancer* 1989;43:250–3.
11. Bartholomew C, Jack N, Edwards J, Charles W, Corbin D, Cleghorn FR, Blattner WA. HTLV-I serostatus of mothers of patients with adult T-cell leukemia and HTLV-I-associated myelopathy/tropical spastic paraparesis. *J Hum Virol* 1998;1: 302–5.
12. Wilks R, Hanchard B, Morgan O, Williams E, Cranston B, Smith ML, Rodgers-Johnson P, Manns A. Patterns of HTLV-I infection among family members of patients with adult T-cell leukemia/ lymphoma and HTLV-I associated myelopathy/tropical spastic paraparesis. *Int J Cancer* 1996; 65:272–3.
13. Seiki M, Eddy R, Shows TB, Yoshida M. Nonspecific integration of the HTLV provirus genome into adult T-cell leukaemia cells. *Nature* 1984; 309:640–2.
14. Wattel E, Vartanian JP, Pannetier C, Wain-Hobson S. Clonal expansion of human T-cell leukemia virus type I-infected cells in asymptomatic and symptomatic carriers without malignancy. *J Virol* 1995;69: 2863–8.
15. Etoh K, Tamiya S, Yamaguchi K, Okayama A, Tsubouchi H, Ideta T, Mueller N, Takatsuki K, Matsuoka M. Persistent clonal proliferation of human T-lymphotropic virus type I-infected cells in vivo. *Cancer Res* 1997;57:4862–7.
16. Cavrois M, Leclercq I, Gout O, Gessain A, Wain-Hobson S, Wattel E. Persistent oligoclonal expansion of human T-cell leukemia virus type 1-infected circulating cells in patients with Tropical spastic paraparesis/HTLV-1 associated myelopathy. *Oncogene* 1998;17:77–82.
17. Gillet NA, Malani N, Melamed A, Gormley N, Carter R, Bentley D, Berry C, Bushman FD, Taylor GP, Bangham CR. The host genomic environment of the provirus determines the abundance of HTLV-1-infected T cell clones. *Blood* 2011;117: 3113–22.
18. Tanaka G, Okayama A, Watanabe T, Aizawa S, Stuver S, Mueller N, Hsieh CC, Tsubouchi H. The clonal expansion of human T lymphotropic virus type 1-infected T cells: a comparison between seroconverters and long-term carriers. *J Infect Dis* 2005;191: 1140–7.
19. Takenouchi H, Umeki K, Sasaki D, Yamamoto I, Nomura H, Takajo I, Ueno S, Umekita K, Kamihira S, Morishita K, Okayama A. Defective human T-lymphotropic virus type 1 provirus in asymptomatic carriers. *Int J Cancer* 2010; 128:1335–43.
20. Okayama A, Stuver S, Matsuoka M, Ishizaki J, Tanaka G, Kubuki Y, Mueller N, Hsieh CC, Tachibana N, Tsubouchi H. Role of HTLV-1 proviral DNA load and clonality in the development of adult T-cell leukemia/lymphoma in asymptomatic carriers. *Int J Cancer* 2004; 110:621–5.
21. Iwanaga M, Watanabe T, Utsunomiya A, Okayama A, Uchimaru K, Koh KR, Ogata M, Kikuchi H, Sagara Y, Uozumi K, Mochizuki M, Tsukasaki K, et al. Human T-cell leukemia virus type I (HTLV-1) proviral load and disease progression in asymptomatic HTLV-1 carriers: a nationwide prospective study in Japan. *Blood* 2010;116:1211–9.
22. Iga M, Okayama A, Stuver S, Matsuoka M, Mueller N, Aoki M, Mitsuya H, Tachibana N, Tsubouchi H. Genetic evidence of transmission of human T cell lymphotropic virus type 1 between spouses. *J Infect Dis* 2002;185:691–5.
23. Tamiya S, Matsuoka M, Etoh K, Watanabe T, Kamihira S, Yamaguchi K, Takatsuki K. Two types of defective human T-lymphotropic virus type I provirus in adult T-cell leukemia. *Blood* 1996;88: 3065–73.
24. Kamihira S, Sugahara K, Tsuruda K, Minami S, Uemura A, Akamatsu N, Nagai H, Murata K, Hasegawa H, Hirakata Y, Takasaki Y, Tsukasaki K, et al. Proviral status of HTLV-1 integrated into the host genomic DNA of adult T-cell leukemia cells. *Clin Lab Haematol* 2005;27: 235–41.
25. Ohshima K, Kikuchi M, Masuda Y, Kobari S, Sumiyoshi Y, Eguchi F, Mohtai H, Yoshida T, Takeshita M, Kimura N. Defective provirus form of human T-cell leukemia virus type I in adult T-cell leukemia/lymphoma: clinicopathological features. *Cancer Res* 1991;51:4639–42.
26. Miyazaki M, Yasunaga J, Taniguchi Y, Tamiya S, Nakahata T, Matsuoka M. Preferential selection of human T-cell leukemia virus type 1 provirus lacking the 5' long terminal repeat during oncogenesis. *J Virol* 2007;81: 5714–23.
27. Korber B, Okayama A, Donnelly R, Tachibana N, Essex M. Polymerase chain reaction analysis of defective human T-cell leukemia virus type I proviral genomes in leukemic cells of patients with adult T-cell leukemia. *J Virol* 1991;65: 5471–6.
28. Yoshida M. Multiple viral strategies of HTLV-1 for dysregulation of cell growth control. *Annu Rev Immunol* 2001;19: 475–96.
29. Mueller N, Okayama A, Stuver S, Tachibana N. Findings from the Miyazaki

Cohort Study. *J Acquir Immune Defic Syndr Hum Retrovirol* 1996;13(Suppl 1): S2–7.
30. Seiki M, Hattori S, Hirayama Y, Yoshida M. Human adult T-cell leukemia virus: complete nucleotide sequence of the provirus genome integrated in leukemia cell DNA. *Proc Natl Acad Sci USA* 1983;80: 3618–22.
31. Kent WJ. BLAT—the BLAST-like alignment tool. *Genome Res* 2002;12: 656–64.
32. Roucoux DF, Wang B, Smith D, Nass CC, Smith J, Hutching ST, Newman B, Lee TH, Chafets DM, Murphy EL. A prospective study of sexual transmission of human T lymphotropic virus (HTLV)-I and HTLV-II. *J Infect Dis* 2005;191:1490–7.
33. Kannagi M. Immunologic control of human T-cell leukemia virus type I and adult T-cell leukemia. *Int J Hematol* 2007; 86:113–7.
34. Matsuoka M, Jeang KT. Human T-cell leukaemia virus type 1 (HTLV-1) infectivity and cellular transformation. *Nat Rev Cancer* 2007;7:270–80.

Int J Hematol (2012) 95:399–408
DOI 10.1007/s12185-012-1020-2

ORIGINAL ARTICLE

Heterogeneity in clonal nature in the smoldering subtype of adult T-cell leukemia: continuity from carrier status to smoldering ATL

Shimeru Kamihira · Masako Iwanaga · Yuko Doi · Daisuke Sasaki · Sayaka Mori · Kazuto Tsurda · Kazuhiro Nagai · Naoki Uno · Hiroo Hasegawa · Katsunori Yanagihara · Yoshitomo Morinaga · Kunihiro Tsukasaki · Hiroaki Taniguchi

Received: 1 November 2011 / Revised: 24 January 2012 / Accepted: 24 January 2012 / Published online: 28 March 2012

Abstract To better understand indeterminate HTLV-1 carriers and smoldering (SM) subtype of adult T-cell leukemia (ATL), HTLV-1 proviral integrated status, proviral load (PVL) and ATL-related biomarkers were examined in 57 smoldering cases, including unusual carriers with a percentage of ATL-like cells. We found that according to Southern blot hybridization analytic features, 28 patients with SM ATL could be divided into 3 groups consisting of 16 (57.4%) patients with a monoclonal band, 6 (21.4%) with oligoclonal bands and the remaining 6 with smears. Although no clinical differences were observed among the 3 SM subtypes, HTLV-1-infected CD4 T-cell counts increased in order of poly-, oligo- and monoclonal subtypes. This trend began in the carrier stage and also was observed in PVL, CD25 and CCR4, indicating that a clone consisting of leukemic phenotypic cells was continuously growing. Moreover, the antigen modulation rates of CD26 and CD7 and the increasing rate of CD25 and CCR4 cells were closely correlated to growing clonal size, indicating that these markers had the possibility to predict a monoclonal band. In particular, CD26 or the ratio of CD26/CD25 had a validity differential for leukemic nature and predictive detection of clonal band. Conclusively, the present study shows that smoldering ATL is heterogeneous in the leukemogenic process, and the behavior of CD26 plays a central role in the evolution from early occult to overt smoldering ATL.

Keywords ATL · HTLV-1 · Provirus · Southern blot · Leukemogenesis

Abbreviations

HTLV-1	Human T-cell leukemia virus type-1
ATL	Adult T-cell leukemia
SBH	Southern blotting hybridization
PMNC	Peripheral blood mononuclear cell
LDH	Lactate dehydrogenase
sIL-2R	Soluble-interleukin-2 receptor

Introduction

Human T-cell leukemia virus type 1 (HTLV-1) was found to be a causative retrovirus of a T-cell malignancy, designated as adult T-cell leukemia (ATL) [1, 2]. All ATL cells, without exception, carry the HTLV-1 provirus in the same genomic site in each case, indicating that provirus insertion is an excellent biomarker for the cellular clonality of ATL and the integrated provirus can be used as the proviral load (PVL) [3] to estimate viral and cellular burden. Proof of clonality is essential for a diagnosis of malignant neoplasm, but it should be noted that HTLV-1-infected cells also are clonally expanded to maintain

S. Kamihira (✉) · Y. Doi · D. Sasaki · S. Mori · K. Tsurda · K. Nagai · N. Uno · H. Hasegawa · K. Yanagihara · Y. Morinaga
Central Diagnostic Laboratory of Nagasaki University Hospital, Nagasaki University Graduate School of Biomedical Sciences, 1-7-1 Sakamoto, Nagasaki 852-8501, Japan
e-mail: kamihira@nagasaki-u.ac.jp

S. Kamihira · K. Nagai · N. Uno · H. Hasegawa · K. Yanagihara · Y. Morinaga
Department of Laboratory Medicine, Nagasaki University Graduate School of Biomedical Sciences, 1-7-1 Sakamoto, Nagasaki 852-8501, Japan

M. Iwanaga · K. Tsukasaki · H. Taniguchi
Department of Hematology, Nagasaki University Graduate School of Biomedical Sciences, 1-7-1 Sakamoto, Nagasaki 852-8501, Japan

persistent infection [2, 4]. Thus, changes in the abundance of HTLV-1-infected cell clones play an important role in persistent infection and ATL leukemogenesis. The clonality of provirus-carrying cells is usually demonstrated by Southern blot hybridization (SBH). However, since the detection sensitivity of this assay is limited (about 5%) [5, 6], it is unavailable for samples including small clones with 5% or fewer monoclonal cell populations.

Recently, we have had many opportunities to see patients with smoldering ATL and unusual carriers with high HTLV-1 PVL or with a proportion of ATL-like cells. We sometimes struggle to distinguish such borderline cases between carriers and smoldering ATL. ATL cells phenotypically resemble Treg cells expressing CD4, CCR4 and CD25. On the other hand, ATL cells aberrantly express 100 or more cell surface receptors and ligands [7, 8]. Such aberrantly expressed receptors consist mainly of natural, adaptive and ectopic types, some of which are considered to be involved in leukemogenesis [9]. In particular, down-regulation of CD3, CD7 and CD26 are observed during the early phase of leukemogenesis [9]. However, little is known about the behavior of cells concurrently expressing CD4, CD25, CCR4 and CD26 in the carrier to SM stages using in vivo practical samples. Accordingly, to better understand indeterminate carriers and smoldering ATL, the present study was focused on the implication between the SBH features reflecting clone size and cellular changes in phenotype and number. In particular, CD26 is noted to be one of the prodromal cellular changes, because the down-regulation of CD26 begins in the carrier stage and persists continuously till the completion of ATL.

Materials and methods

White blood cell counts, morphological data, serum lactate dehydrogenase (LDH) activity and soluble interleukin-2 receptor (sIL-2R) were used from routine laboratory data. Peripheral blood samples were collected from our ATL and HTLV-1 carrier clinic, consisting of 28 patients with smoldering ATL carrying 5% or more ATL-like cells in blood, 12 unusual carriers with around 5% ATL-like cells, and 17 common (healthy) carriers. Thirty-four samples from patients with leukemic chronic or acute ATLs were used as a positive control. Morphological evaluation was microscopically conducted by hematological specialists.

High-molecular-weight DNA was extracted from peripheral blood mononuclear cells (PMNC) using a QIAmp DNA Blood Mini Kit (Qiagen GmbH, Hilden Germany). PVL was quantified by LightCycler Technology (Roche Diagnostic K.K., Tokyo, Japan) using hydro-probes and previously described primers [10–12]. Normalization was done using the β-globin gene and the PVL was expressed as copy number per 10^4 cells or percent for PMNC. This study was done under the approval of our institutional board.

Clone assay of SBH

SBH analysis was performed by a method described previously with modification, using 7 mixtures of probes covering the total region of the digoxigenined provirus and the restriction enzymes of EcoR-1 and Pst-1 [13, 14]. Pst-1 cuts 4 sites of the provirus, but Eco-R1 cannot cut within the provirus. Therefore, to determine clonally related sharp band or polyclonally related smear bands, Eco-R1 digestive genomic fragments were used. To assay clonality accurately, we monitored 1.5, 3 and 5% clonal cell controls every time. Band patterns were estimated using a densitometer (Fujifilm Life Science, Science Lab 2005, and Tokyo, Japan).

Flow cytometry analysis for cell surface antigens

The positive rate for CD3, CD4, CD7, CD25, CD26 and CCR4 was measured by a routine method using whole blood according to the manufacturer's instructions (BD FACSCato-II, Nixon BD. Inc, Tokyo, Japan). The association between CD7 and CD26 antigen modulation and the positivity of CD4, CD25 and CCR4 cells was assessed by using the four-color staining method according to the manufacturer's instructions. Co-expression with CD4, CD25, CCR4 and CD26 was assessed by a four-color flow cytometric method using CD26-FITC, CD4-PerCP, CD25-APC and CCR4-PE. The rate (%) of $CD4^{(+)}CD25^{(+)}CCR4^{(+)}$ cells relative to all CD4 cells and the co-expression rate of CD26 with $CD4^{(+)}CD25^{(+)}CCR4^{(+)}$ cells was measured according to the BD FACSCato-II protocol (BD, Inc., Tokyo, Japan).

Statistical analysis

Data are expressed mainly as the median and analyzed using the Mann–Whitney test. P value of below 0.05 was considered to be statistically significant. Analyses were performed with Stat Flex version 6.5 software packages (Artech Inc., Osaka, Japan).

Results

Classification features of band patterns using a densitometer

The band patterns in SBH analysis using Eco-R1-digestive genomic fragments were mainly estimated by a densitometer graph. The densitometer graphs equivalent to band

status are classified into five patterns (Fig. 1a): patterns-1 and -2 are light and dense smear bands with no difference in staining density; pattern-3 is a hill ridge, irregular shape with vertical stripes or a low and broad projection with smear bands; pattern-4 is a low/sharp peak type; and pattern-5 is a sharp high peak. In vivo clonal status of the five patterns based on SBH features, as shown in Fig. 1b, is considered to correspond to few small clones in pattern (P)-1, many small clones with few growing clones in P-2, oligoclones of a detection limit in P-3, and clearly detectable monoclone(s) with various background clonal status in P-4 and 5.

SBH analysis allocated 57 cases to 17 of P-1, 11 of P-2, 12 of P-3, 6 of P-4 and 11 of P-5. The relations between intra- or inter-disease status and the band patterns are summarized in Table 1. Consequently, smoldering ATL was the most heterogeneous for SBH patterns; 16 (57.1%) of 28 smoldering ATLs were P-4 and -5 (large clone consisting of at least 5% monoclonal cells), while the remaining 12 (42.9%) were P-1, -2 and -3 (equivalent to polyclonal or oligoclonal band). Actually, Fig. 2 is an interesting example of an SM subtype showing dense smear bands and abnormal cells with an aberrant phenotype of 73% CD4, 77% CD25 and 21% CD26.

Cyto-oncological characteristics of the three SM subtypes

To characterize ATL-related biomarkers in the three subtypes of SM, the findings were comprehensively compared with those of healthy carriers, unusual carriers and patients with chronic ATL (Table 2). First, clonal expansion-associated biomarkers, such as PVL, HTLV-1-infected CD4 T-cell counts in 1 μL peripheral blood and the serum level of sIL-2R increased regularly in the order of poly-, oligo- and monoclonal SM subtypes. Figure 3 shows the line graphs on increasing fold (rate) of PVL and total lymphocyte, all CD4 T-cell and HTLV-1-infected CD4 T-cell counts converted from Table 2. The graph shows two distinctive patterns (solid lines of PVL and infected CD4 T-cell vs. broken lines of total lymphocyte and all CD4 T-cell). In contrast to the horizontal part of the broken lines, the solid lines are gradually elevated, meaning that the provirus-carrying CD4 T-cells gradually increase

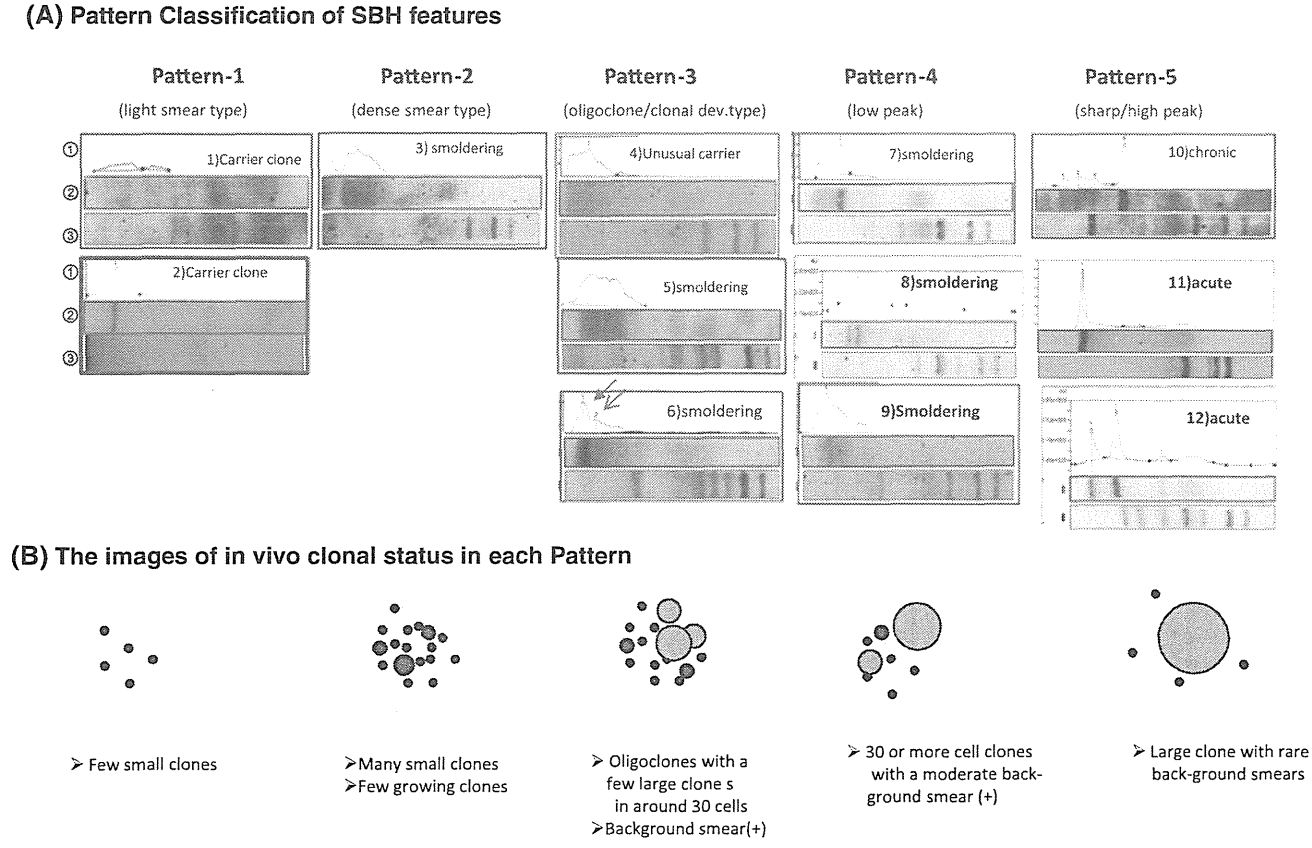

Fig. 1 **a** The densitometry patterns for HTLV-1 proviral integration status according to SBH band features using a restrictive enzyme of Eco-R1 and representative cases. Subjects were mainly classified into five patterns according to densitometer images. ① Densitometry graph. ② SBH analysis for Eco-R1-digestive genomic fragments. ③ SBH analysis for Pst-1-digestive genomic fragments. **b** The image of in vivo clonal status in each pattern

Table 1 The pattern distribution of SBH features in intra- and inter-diseases

	Smear band		Oligoclonal bands	Monoclonal bands		Total
	P-1	P-2	P-3	P-4	P-5	
Common carriers	11	5	0	0	(1)[a]	17
Unusual carriers	5	1	6	0	0	12
Smoldering ATL	1	5	6	6	10	28

The criteria of the classification is explained in the text. P-1, P-2, P-3, and P-4 and P-5 generally correspond to light smears, dense smears, oligoclonal bands and monoclonal bands, respectively. Of leukemic type ATL, including the chronic and acute type, SBH features in smoldering ATL were the most heterogeneous

Common carriers HTLV-1-seropositive individuals without any HTLV-1-associated disorders

Unusual carriers those who have clinico-cytological findings similar to that of the smoldering subtype of ATL

[a] Carrier clone

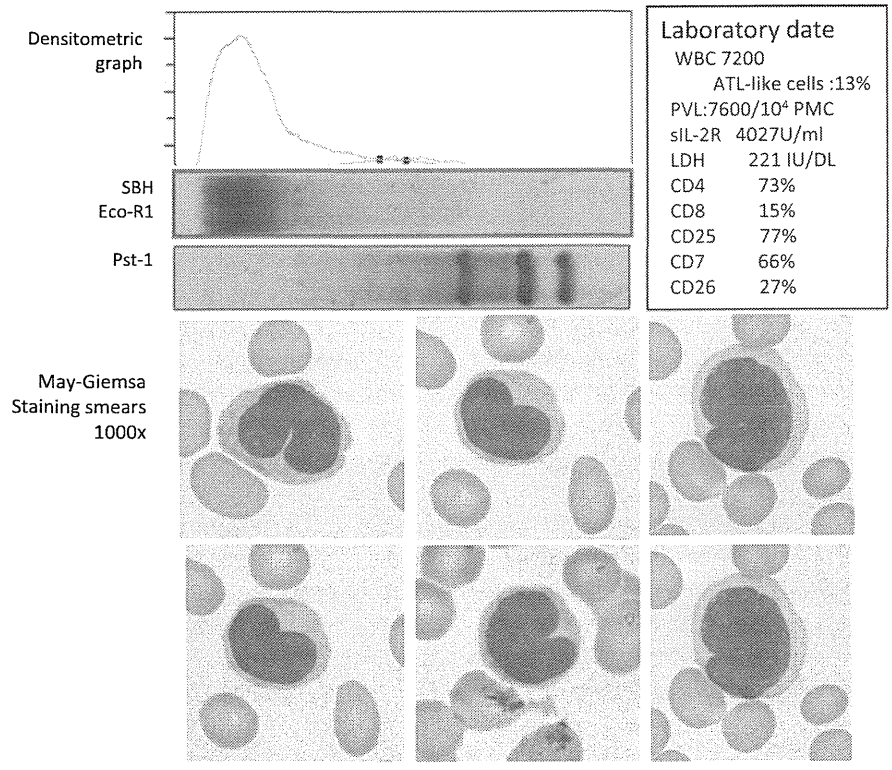

Fig. 2 A representative case presentation of the polyclonal smoldering subtype (SM) showing a polyclonal dense smear in SBH analysis and the smoldering subtype with full hematological criteria

regardless of the almost stable counts of non-infected CD4 T-cells during the entire period of smoldering ATL.

The positive values of CD4, CD25, CCR4, CD7 and CD26 subsets (%) were observed to change continuously and concurrently in the order of common carriers, unusual carriers, polyclonal SM, oligoclonal SM and monoclonal SM. In order to interpret these data in detail, a line graph was used (Fig. 4). CCR4 and CD25 cells increased concurrently and sharply from the common carrier stage to the oligoclonal stage. The down-regulation of CD26 was initiated in the unusual carrier stage and kept falling continuously by chronic stage. The fluctuations of CD4 and CD26 showed an opposing trend, and the interval between CD4 and CD26 (solid triangle and gray circle) gradually enlarged with the increasing cell number of 32, 54, 115 and 163 cells. Such behavior of CD26 was expected to play a central role in budding of ATL in the early stage of multistep leukemogenesis.

Clinico-oncological usefulness of CD26

From the results described above, CD26 appears to be closely associated with the evolution of SM. In contrast to characteristic phenotypes in overt ATL cells, those of

Table 2 Comparison of the measurement value (mean) of ATL-related biomarkers among the polyclonal, oligoclonal and monoclonal SM subtypes

	Carrier stage		Smoldering stage			Chronic
	Common	Unusual	Polyclonal	Oligoclonal	Monoclonal	
PVL (%)	5.9	17.9	22.6*	28.0	39.3*	78.3
Total Ly counts	1750	1950	2308	1732	2306	7659
All CD4 T-cell	786	882	1570	1513	1377	7220
Infected CD4	102	330	480*	628	744*	8346
LDH (IU/mL)	199	200	222	186	179	257
sIL-2R (U/mL)	868	765	1425	1877	1887	6106
CD4 (%)	43	48	52	55	56	79
CD25 (%)	14	22	32	45	44	75
CCR4 (%)	14	25	38*	50	58**	76
CD7 (%)	63	65	70	47	50	11
CD26 (%)	43	41	41*	28	22**	7

Statistically significant ($P < 0.05$) between * and ** in PVL, infected CD4 cell number, CCR4 (%) and CD26 (%)

HTLV-1-infected CD4 T-cell number/1 μL p-blood = total Ly counts × CD4%/100 × PVL (%/100)

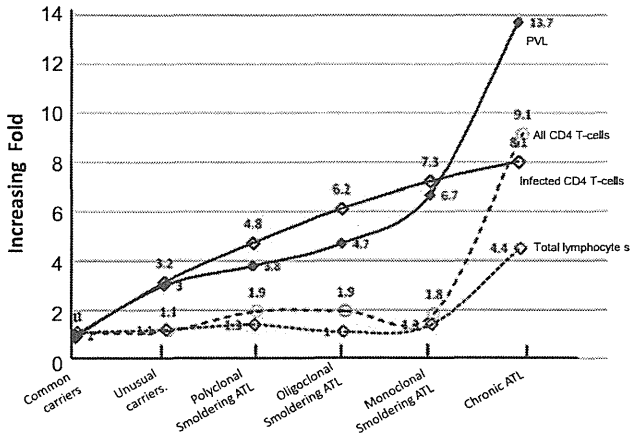

Fig. 3 The difference in the line-graph patterns between HTLV-1-infected and uninfected cells. PVL and infected CD4 T-cell counts gradually increased from the early carrier stage to the last stage of smoldering, while the HTLV-1-uninfected cell population was stable, indicating that the discrepancy was explained by the infected leukemic clonal expansion alone

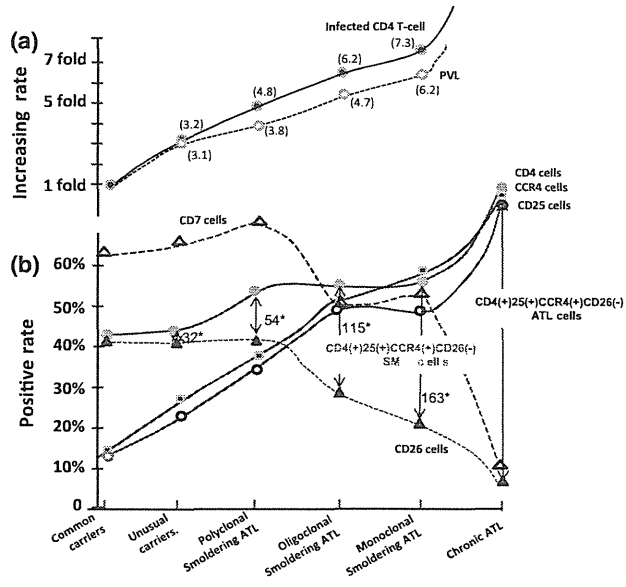

Fig. 4 The rate of change in each ATL-related biomarker. There were two major types of curves; a concurrent increasing type with tumor burden and a decreasing type with aberrant down-regulation. **a** The increasing rate (fold) relative to 102 HTLV-1-infected CD4 T-cells in 1 μL of blood. **b** Comparison of the positive rates in each disease state equivalent to P-1 (common carriers), P-2 (dense smears), P-3 (oligoclonal), and P-4 and P-5 corresponding to the monoclonal phase. *Asterisks* represent predicted $CD4^{(+)}CD26^{(-)}$ cell number equivalent to a major clonal expansion representing the absolute increased tumor burden

occult ATL (SM) cells are now controversial. One of the reasons for this is thought to be the difficulty in identifying SM cells. Therefore, to overcome these problematic issues, a dot-plot graph for CD26 versus CD25 and a four-color staining method were applied. The dots of CD26 and CD25 were mainly clustered into two areas (Fig. 5): 11 of monoclonal SM were clustered into a solid line circle, while oligoclonal and polyclonal SM were widely distributed. On the other hand, carriers were compactly clustered within the broken line circle. This indicates that also the 3 SM subtypes are not always homogeneous in biological character. Since the CD25 versus CD26 dot graph only hinted at the heterogeneity of SM, we examined the clinico-oncological role of CD26 using 3 parameters of HTLV-1-infected cell counts, the CD26/CD25 ratio and SBH features. As shown in Fig. 6, the number of HTLV-1-infected CD4 T-cells was closely correlated to the ratio of

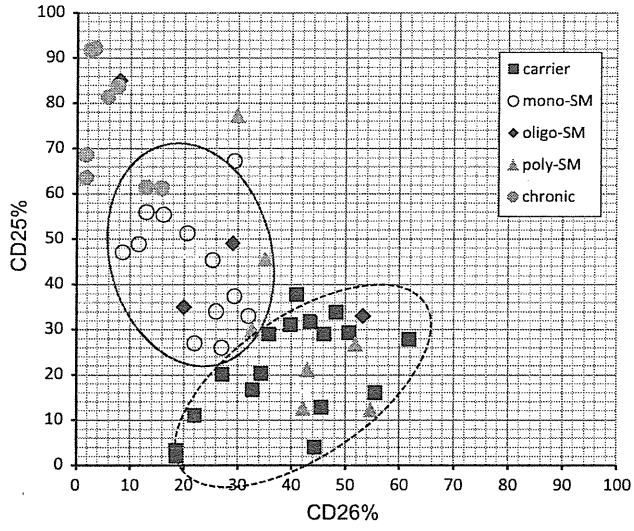

Fig. 5 CD26 versus CD25 twin dot graph, showing that there were two hot areas. The cells clustering in the same area have uniform biocharacteristics. Monoclonal SM was concentrated in the same area, but polyclonal SM and carriers were distributed sparsely and widely. *Red squares within dotted line circle* 3SM subtypes were scattered into both circles

CD26/CD25 ($R^2 = 0.6586$), and the clustering patterns were characteristic.

Samples with monoclonal band were mainly clustered in a high area within 0 to <1 of the *X*-axis. Most other samples were widely distributed in a area of around 1.00–11.00 of the *Y*-axis. Thus, the CD26/CD25 ratio represents the degree of advance in the leukemic process, comparable to the growing level of an ATL cell clone. Actually, this was demonstrated to be an indicator of a monoclonal band using a distribution graph and a receiver operating curve (ROC). That is, as shown in Fig. 7a, the ratios of CD26/CD25 were clearly separated by the presence or absence of a monoclonal band. The ROC analysis gave a high area under the curve (AUC) of 0.90, and sensitivity, specificity, and positive and negative predictive values were 87.0, 83.0, 80.0 and 89.0%, respectively (Fig. 7b), when the ratio of cutoff value (COV) was 1.04. The detective test performances of CD26 and CD7 alone for a monoclonal band were 0.82 and 0.81 AUC, respectively. This simple predictive method as an alternative to the SBH test, which is time- and labor-consuming, may be practically useful.

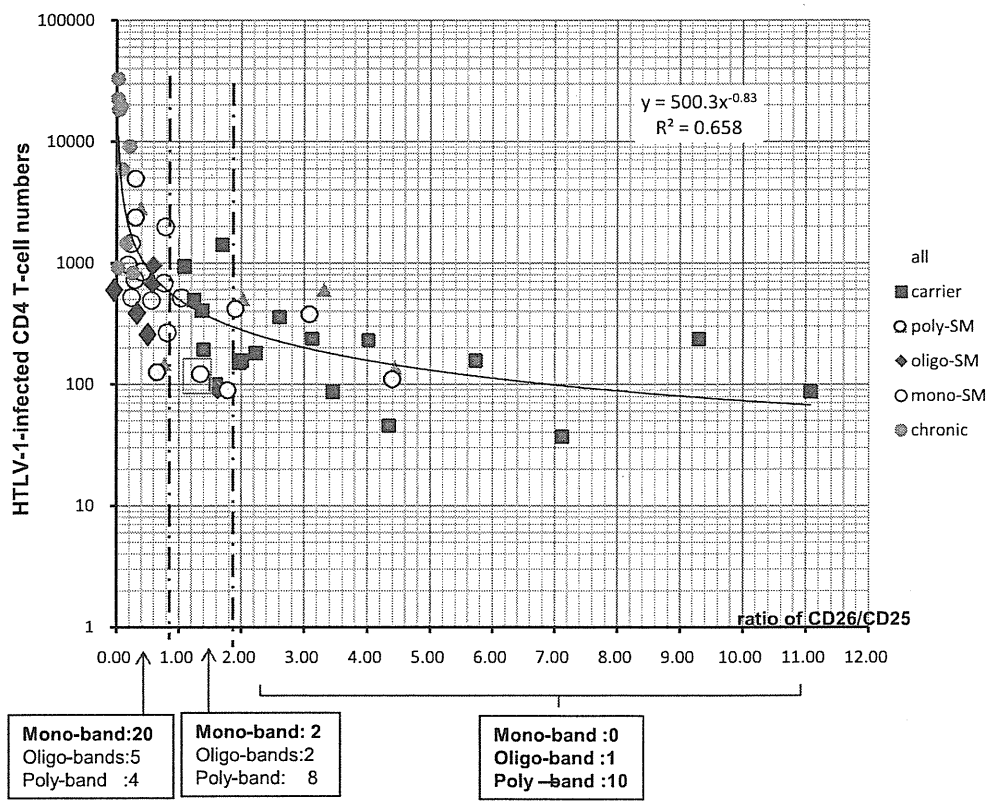

Fig. 6 Three parameter "twin dot-plot graph" between HTLV-1-infected CD4 T-cell numbers and the ratio of CD25/CD26, and the carrier or disease subtypes. Samples with the same band pattern showed a tendency to gather in the same areas bordered by the CD25/26 ratio lines, such as most samples with monoclonal band (momo-band) in an area within 0.00–1.00 of the *X*-axis, and most samples with smears (poly-band) in an area within 1.00–11.00 of the *X*-axis

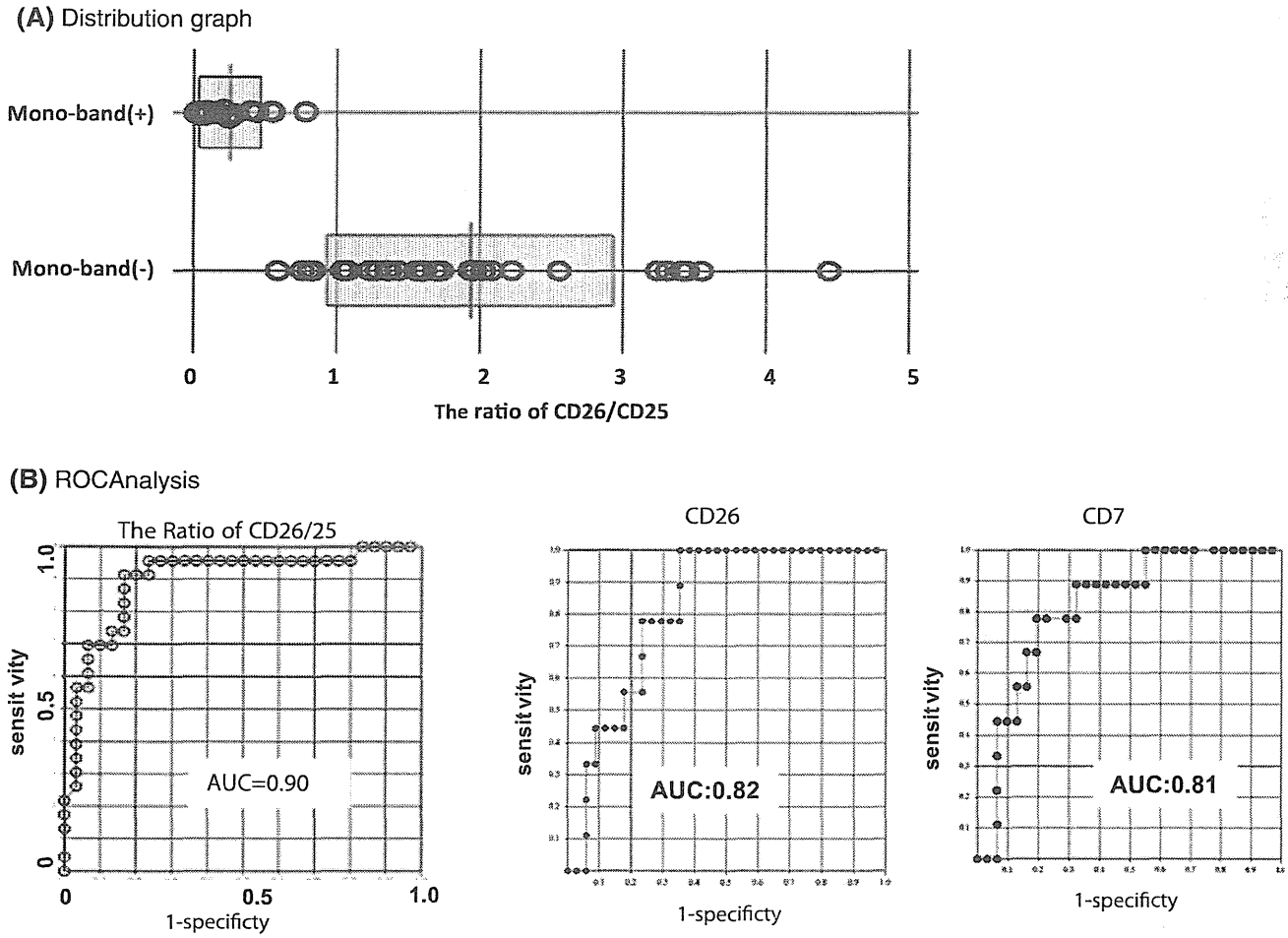

Fig. 7 **a** The distribution graph of each sample with or without a monoclonal band. The median values of mono-band (+) or (−) were 0.32 and 1.98. **b** The receiver operating curve (ROC) analysis

Correlation between down-regulation of CD26 antigens and SBH features

It is known that CD7 and CD26 antigens are lost in chronic and acute ATL cells. The present study revealed that the loss of CD26 antigens was initiated early in the pattern-2 or -3 stages. To confirm whether $CD4^{(+)}$ $CD25^{(+)}$ $CCR4^{(+)}$ cells were concurrently expressed, a four-color staining flow cytometric method for CD4, CD25, CCR4 and CD26 was used (Fig. 8). $CD4^{(+)}$ $CD25^{(+)}$ $CCR4^{(+)}$ cells (P1 square) were 1% or less, of which 75% (0.3% of total CD4 cells) were CD26 negative and 25% were CD26 positive in a healthy individual seronegative for HTLV-1 (case 1). That is, the $CD25^{(-)}/CD26^{(+)}$ ratio was 3.0. On the other hand, the ratio in common carriers and SM subtypes was about 3.0–10.0 (cases 2–4) and 10 or more (cases 5–9), respectively. This phenomenon regarding the loss of CD26 antigens was observed in other ATL cells [20].

Discussion

More than 35 years have passed since ATL was found and HTLV-1 was identified as its causative virus several years later. After that, a better molecular understanding of ATL pathology has been advancing. However, at the forefront of clinical practice, many problematic issues, such as a correct diagnosis of smoldering ATL, discrimination from unusual carriers with a percentage of ATL-like cells and promising therapeutic strategies, remain unclear. Recently, understanding of ATL pathology has deepened, but there is no point of contact between clinical and molecular aspects.

The results of the present study revealed that SM was heterogeneous in clonally related SBH features (mainly clone size) and lymphocyte subset profiles. We here designated such cases as monoclonal, oligoclonal and polyclonal smoldering (SM) subtypes. Although there was no difference in clinical manifestations, increase of only

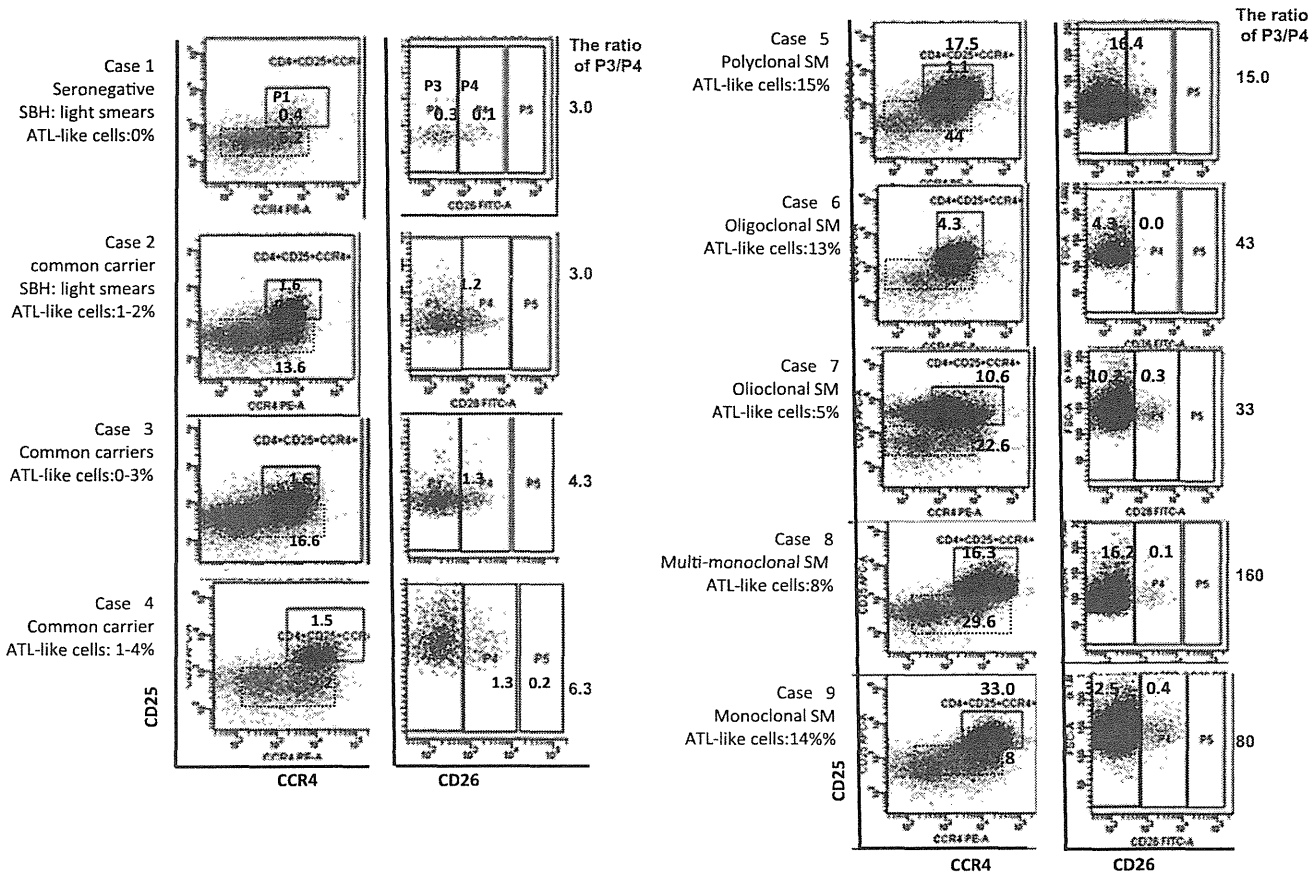

Fig. 8 Four-color flow cytometry for CD4, CD25, CCR4 and CD26. After CD4 gating, gating-CD4 T-cells were developed into a cytograph (a CCR4 = *X*-axis, and CD25 = *Y*-axis), and then P1 gating cells were developed into a cytograph (b CD26 down-regulation positive (*blue* P3 area meaning loss of CD26 antigen) or negative (*red* P4 area)

HTLV-1 provirus-carrying cells with a phenotype of $CD4^+CD25^+CCR4^+CD26^-$ was characteristic, regardless of the stable lymphocyte counts. Moreover, the ratio of CD26/CD25 was defined to be useful as an indicator of the grade of advance into ATL. Such findings were observed partially in unusual carriers with oligoclonal bands. These suggest that the expansion of leukemic clone begins in the unusual carrier stage and reaches large clone detected by SBH analysis in the SM stage. Thus, continuous changes of all ATL-related biomarkers would be explained by growing leukemic clonal cell population [15]. This is easily understood by a diagram shown in Figs. 3 and 4, which was derived from the increase of absolute CD4 T-cells infected by HTLV-1. The SM period seems to oncologically mean one of the turning points for multi-step leukemogenesis of ATL.

Now, it is interesting to develop such a subtype manifestations. Although clinical over-diagnosis cannot be completely neglected, there are in fact such cases with a highly dense smear for Eco-R1 genomic fragments and internal bands for Pst-1 genomic fragments, like the case in Fig. 2. As a possibility, a cluster of small clones may work co-operatively to develop SM manifestations. Subsequently, this appears to give rise to frequently multiclonal ATL and genomic diversity of leukemic clones [16].

Another interest is the behavior of CCR4, CD7 and CD26. So far, little is known about CD26 associated with ATL pathology. CD26/dipeptide peptidase IV (DPPIV), which is an antigenic enzyme expressed on the surface of most cell types, suppresses the development of cancer and tumors. CD26 plays an important role in tumor biology, and is useful as a marker for various cancers [17–19]. Now, why would down-regulation of CD26 first occur? The down-regulation preceding the increase in HTLV-1-infected CD4 T-cells may be indispensable to an environment for growing immature ATL cells. On the other hand, down-regulation of CD7, a glycoprotein member of the immunoglobulin (Ig) superfamily, is also one of the most commonly seen antigenic aberrations in T-lymphoproliferative disorders, but there is no specificity for malignant cell types, including a variety of reactive conditions [20, 21]. The changes in expression of CCR4 and CD26 may be the results of transformation.

Furthermore, to reveal other roles of CD26, statistical methodology and a dot plot were used. Consequently, two twin dot-plot graphs of CD25 versus CD26, and HTLV-1-CD4 T-cell number versus the ratio of CD26/CD25 revealed that the ratio of CD26/CD25 is useful as a surrogate marker for the prediction of the provirus clonal status. When the COV of the ratio is 1.04, the diagnostic validity is 87.0% in sensitivity and 83% in specificity. However, the ratio of CD26/CD25 in polyclonal SM was widely distributed, indicating that the polyclonal SM was distinctive from the other two subtypes of oligo- and monoclonal SM. This simple predictive method, alternative to the SBH test which is time- and labor-consuming, may be practically useful for screening in rapid turn-around test or epidemiological mass test.

Finally, using four-color flow cytometry, the usefulness of the CD26 antigen monitor was verified in actual cases. The antigen status was evaluated as the ratio of $CD26^{(-)}$ versus $CD26^{(+)}$ within a fraction of $CD4^{(+)}CD25^{(+)}CCR4^{(+)}$ cells. The ratio went up with increases in the $CD4^{(+)}CD25^{(+)}CCR4^{(+)}$ cell populations, reflecting occult ATL cells or transforming cells. In the present study, the border line of the ratio between carriers and patients with SM was about 10.0. That is, if the $CD26^{(-)}$:$CD26^{(+)}$ ratio is 10 or more, the case is predicted to be smoldering ATL.

Taken together, the present study showed that smoldering ATL was heterogeneous in a clone size and the quality of its constituent cells. This suggests that it is relevant to classify the current smoldering ATL into two subtypes of SM with or without a monoclonal band. Indeterminate HTLV-1 carriers and smoldering ATL can be discriminated according to the patterns of SBH densitometer images and CD26 antigen status. Moreover, CD26 is expected to be used as a novel biomarker for prediction of clonal bands and discrimination of carriers or SM subtypes. CD26 may become one of the central molecules in understanding the early leukemogenic process.

Acknowledgments This work was supported by the Japanese Government, Kakenn B No. 21390182. This study was performed as a cooperative study, mainly organized by SK and with the other authors YD, SD, MO, KT, KN, NU, HH, KY, KT and HT.

Conflict of interest The authors have no conflict of interest.

References

1. Poiesz BJ, Ruscetti FW, Gazdar AF, Robbert Gallo C. Detection and isolation of type C retrovirus particles from fresh and cultured lymphocytes of patients with cutaneous T-cell lymphoma. Proc Natl Acad Sci USA. 1980;77(12):7415–9.
2. Matsuoka M, Jeang KT. Human T-cell leukaemia virus type 1 (HTLV-1) infectivity and cellular transformation. Nat Rev Cancer. 2007;7(4):270–80.
3. Yoshida M. Discovery of HTLV-1, the first human retrovirus, its unique regulatory mechanisms, and insights into pathogenesis. Oncogene. 2005;24(39):5931–7.
4. Tanaka G, Okayama A, Watanabe T, Aizawa S, Stuver S, Mueller N, Hsieh CC, Tsubouchi H. The clonal expansion of human T lymphotropic virus type 1-infected T cells: a comparison between seroconverters and long-term carriers. J Infect Dis. 2005;91(7):1140–7.
5. Kamihira S, Sugahara K, Tsuruda K, Minami S, Uemura A, Akamatsu N, Nagai H, Murata K, Hasegawa H, Hirakata Y, Takasaki Y, Tsukasaki K, Yamada Y. Proviral status of HTLV-1 integrated into the host genomic DNA of adult T-cell leukemia cells. Clin Lab Haematol. 2005;27(4):235–41.
6. Sugahara K, Yamada Y. Southern blot hybridization analysis for lymphoid neoplasms. Rinsho Byori. 2000;48(8):702–7.
7. Kamihira S, Sohda H, Atogami S, Fukushima T, Toriya K, Miyazaki Y, Ikeda S, Yamada Y, Tomonaga M. Unusual morphological features of adult T-cell leukemia cells with aberrant immunophenotype. Leuk Lymphoma. 1993;12(1–2):123–30.
8. Maeda T, Yamada Y, Moriuchi R, Sugahara K, Tsuruda K, Joh T, Atogami S, Tsukasaki K, Tomonaga M, Kamihira S. Fas gene mutation in the progression of adult T cell leukemia. J Exp Med. 1999;189(7):1063–71.
9. Tsuji T, Sugahara K, Tsuruda K, Uemura A, Harasawa H, Hasegawa H, Hamaguchi Y, Tomonaga M, Yamada Y, Kamihira S. Clinical and oncologic implications in epigenetic down-regulation of CD26/dipeptidyl peptidase IV in adult T-cell leukemia cells. Int J Hematol. 2004;80(3):254–60.
10. Sasaki D, Doi Y, Hasegawa H, Yanagihara K, Tsukasaki K, Iwanaga M, Yamada Y, Watanabe T, Kamihira S. High human T cell leukemia virus type-1 (HTLV-1) provirus load in patients with HTLV-1 carriers complicated with HTLV-1-unrelated disorders. Virol J. 2010;7:81.
11. Kamihira S, Dateki N, Sugahara K, Yamada Y, Tomonaga M, Maeda T, Tahara M. Real-time polymerase chain reaction for quantification of HTLV-1 proviral load: application for analyzing aberrant integration of the proviral DNA in adult T-cell leukemia. Int J Hematol. 2000;72(1):79–84.
12. Kamihira S, Dateki N, Sugahara K, Hayashi T, Harasawa H, Minami S, Hirakata Y, Yamada Y. Significance of HTLV-1 proviral load quantification by real-time PCR as a surrogate marker for HTLV-1-infected cell count. Clin Lab Haematol. 2003;25(2):111–7.
13. Uemura A, Sugahara K, Nagai H, Murata K, Hasegawa H, Hirakata Y, Tsukasaki K, Yamada Y, Kamihira S. An ATL cell line with an IgH pseudo-rearranged band pattern by Southern blotting: a pitfall of genetic diagnosis. Lab Hematol. 2005;11(1):8–13.
14. Shimoyama M. Diagnostic criteria and classification of clinical subtypes of adult T-cell leukaemia-lymphoma. A report from the Lymphoma Study Group (1984–87). Br J Haematol. 1991;79(3):428–37.
15. Gillet NA, Malani N, Melamed A, Gormley N, Carter R, Bentley D, Berry C, Bushman FD, Taylor GP, Bangham CR. The host genomic environment of the provirus determines the abundance of HTLV-1-infected T-cell clones. Blood. 2011;117(11):3113–22.
16. Ariyama Y, Mori T, Shinomiya T, Sakabe T, Fukuda Y, Kanamaru A, Yamada Y, Isobe M, Seto M, Nakamura Y, Inazawa J. Chromosomal imbalances in adult T-cell leukemia revealed by comparative genomic hybridization: gains at 14q32 and 2p16-22 in cell lines. J Hum Genet. 1999;44(6):357–63.
17. Tian Y, Kobayashi S, Ohno N, Isobe M, Tsuda M, Zaike Y, Watanabe N, Tani K, Tojo A, Uchimaru K. Leukemic T cells are specifically enriched in a unique CD3 (dim) CD7 (low) subpopulation of CD4(+) T cells in acute-type adult T-cell leukemia. Cancer Sci. 2011;102(3):569–77.

18. Kelemen K, Guitart J, Kuzel TM, Goolsby CL, Peterson LC. The usefulness of CD26 in flow cytometric analysis of peripheral blood in Sézary syndrome. Am J Clin Pathol. 2008;129(1): 146–56.
19. Sato T, Yamochi T, Yamochi T, Aytac U, Ohnuma K, McKee KS, Morimoto C, Dang NH. CD26 regulates p38 mitogen-activated protein kinase-dependent phosphorylation of integrin beta1, adhesion to extracellular matrix, and tumorigenicity of T-anaplastic large cell lymphoma Karpas 299. Cancer Res. 2005; 65(15):6950–6.
20. Narducci MG, Scala E, Bresin A, Caprini E, Picchio MC, Remotti D, Ragone G, Nasorri F, Frontani M, Arcelli D, Volinia S, Lombardo GA, Baliva G, Napolitano M, Russo G. Skin homing of Sézary cells involves SDF-1-CXCR4 signaling and down-regulation of CD26/dipeptidylpeptidase IV. Blood. 2006;107(3):1108–15.
21. Abe M, Uchihshi K, Tsuruda K, Kamihira S. Foxp3 expression on normal and leukemic CD4+CD25+ T-cells implicated in HTLC-1 is inconsistent with Treg cells. Europ J Haematol. 2008;81:209–17.

Jpn. J. Infect. Dis., 65, 334-336, 2012

Short Communicaiton

Xenotropic Murine Leukemia Virus-Related Virus Proviral DNA Not Detected in Blood Samples Donated in Japan

Chieko Matsumoto[1]*, Masashi Igarashi[1], Rika A. Furuta[2], Shigeharu Uchida[1], Masahiro Satake[1], and Kenji Tadokoro[1]

[1]*Japanese Red Cross Society Blood Service Headquarters, Tokyo 135-8521; and* [2]*Japanese Red Cross Kinki Block Blood Center, Osaka 567-0085, Japan*

(Received January 19, 2012. Accepted May 8, 2012)

SUMMARY: The xenotropic murine leukemia virus-related virus (XMRV) was first described as a novel human gammaretrovirus in prostate tumor tissues and was reported to be found in blood, suggesting the possibility of XMRV transmission via blood transfusion. The *gag* and *env* regions of the XMRV proviral DNA that were detected in 1,030 blood samples collected from the greater Tokyo area were examined by real-time PCR analysis. However, XMRV infection was not found in the samples; this suggested that the risk of XMRV transmission via transfusion is very low in Japan.

Xenotropic murine leukemia virus (MLV)-related virus (XMRV) was first described as a novel human gammaretrovirus in prostate tumor tissues in 2006 (1). In 2009, XMRV genomes were detected in 67% (68/101) of chronic fatigue syndrome (CFS) patients (2). However, this finding remains controversial as several research groups failed to confirm the presence of the gammaretrovirus in patients with CFS or prostate cancer (3-5). Moreover, genomic sequences of XMRV were found in 0-3.7% of blood samples obtained from healthy populations (2,3). XMRV can be transmitted via activated lymphocytes and cell-free plasma of individuals who are diagnosed as virus positive by PCR analysis, and XMRV can replicate in prostate carcinoma cell lines (2,6). These findings indicate the possibility of viral transmission via blood transfusion, which poses a great threat. Therefore, we examined the presence of XMRV proviral DNA in samples of donated blood to evaluate the risk of XMRV infection via blood transfusion in Japan. This study was approved by the ethics committee of the Japanese Red Cross Society.

Samples of donated blood (1,030 whole blood samples) from the greater Tokyo area were collected randomly and anonymously from May 2011 to July 2011. The donors comprised of 712 men and 318 women aged 16-66 years. Cellular DNA was purified from the blood samples using a QIAsymphony DNA Midi kit (QIAGEN, Tokyo, Japan). The number of DNA molecules having the human *CD81* gene, which is present as a single-copy gene per haploid genome, was estimated by real-time PCR analysis to examine the quality and concentration of human DNA in the purified DNA molecules. The primers and minor groove binder (MGB)-bound and VIC-labeled probes that were used are shown in Table 1. A DNA sample containing 300,000 copies of the DNA sequences containing the *CD81* gene weights approximately 1 μg. The *gag* and *env* regions of XMRV proviral DNA were amplified by real-time PCR consisting of 45 amplification cycles. The primers for the *gag* region were 419F (forward) (2) and 518R (reverse), and the FAM-labeled MGB probe was 446MGB. The *env* region was detected according to the method described by Groom et al. (5) using the following: forward primer, 6173envF; reverse primer, 6173envR; and the FAM-labeled MGB probe, 6173envMGB. Two real-time PCRs were performed in duplicates for detecting XMRV genome, and approximately 1 μg DNA from a blood sample was used for each reaction. The real-time PCRs were performed using TaqMan Fast Universal PCR Master Mix and PRISM 7900 (Life Technologies, Tokyo, Japan). Each real-time PCR system used standard curves constructed using various numbers of control DNAs. The three kinds of control DNAs were plasmid DNAs with the sequences of the exon 5 of *CD81* gene, the XMRV *gag* region, and the XMRV *env* region, respectively. The DNA fragments cloned into the plasmids were obtained from the PCR products; the PCR products were amplified from human genomic DNA or XMRV proviral DNA that were isolated from 22Rv1 prostate carcinoma cells, a prostate cancer cell line (7). The copy numbers of plasmids were calculated on the basis of the plasmid concentrations in the solutions. Amplification of the *gag* and *env* plasmids at various copy numbers spiked into 1-μg human genomic DNA, which was free of XMRV DNA, showed that the two real-time PCR systems were capable of detecting at least 10 copies of target DNA.

No XMRV proviral DNA was detected in 1,029 of the 1,030 blood samples. Both the *gag* and *env* regions were slightly reactive in only one sample, No. 75, and the copy numbers of the target sequence per reaction were less than 10 in both real-time PCR systems. To confirm the presence of XMRV proviral DNA, nested PCR of the *gag* and *env* regions was performed using on a DNA sample from blood sample No. 75. The primers used in the nested PCR are shown in Table 1. Two and three copies of the plasmids containing the *gag* and *env* regions,

*Corresponding author: Mailing address: Infectious Disease Research Dep. JRC Central Blood Inst. JRC, 2-1-67 Tatsumi, Koto-ku, Tokyo 135-8521, Japan. Tel: +81-3-5534-7522, Fax: +81-3-3521-4137, E-mail: c-matsumoto@jrc.or.jp